African Journal of Pharmacy and Pharmacology

Volume 9 Number 7, 22 February, 2015

ISSN 1996-0816

Academic Journals

ABOUT AJPP

The **African Journal of Pharmacy and Pharmacology (AJPP)** is published weekly (one volume per year) by Academic Journals.

African Journal of Pharmacy and Pharmacology (AJPP) is an open access journal that provides rapid publication (weekly) of articles in all areas of Pharmaceutical Science such as Pharmaceutical Microbiology, Pharmaceutical Raw Material Science, Formulations, Molecular modeling, Health sector Reforms, Drug Delivery, Pharmacokinetics and Pharmacodynamics, Pharmacognosy, Social and Administrative Pharmacy, Pharmaceutics and Pharmaceutical Microbiology, Herbal Medicines research, Pharmaceutical Raw Materials development/utilization, Novel drug delivery systems, Polymer/Cosmetic Science, Food/Drug Interaction, Herbal drugs evaluation, Physical Pharmaceutics, Medication management, Cosmetic Science, pharmaceuticals, pharmacology, pharmaceutical research etc. The Journal welcomes the submission of manuscripts that meet the general criteria of significance and scientific excellence. Papers will be published shortly after acceptance. All articles published in AJPP are peer-reviewed.

Submission of Manuscript

Submit manuscripts as e-mail attachment to the Editorial Office at: ajpp@academicjournals.org. A manuscript number will be mailed to the corresponding author shortly after submission.

The African Journal of Pharmacy and Pharmacology will only accept manuscripts submitted as e-mail attachments.

Please read the **Instructions for Authors** before submitting your manuscript. The manuscript files should be given the last name of the first author.

Editors

Editorial Board

African Journal of Pharmacy and Pharmacology

Table of Contents: Volume 9 Number 7 22 February, 2015

ARTICLES

Research Articles

academicJournals

Vol. 9(7), pp. 190-197, 22 February, 2015
DOI: 10.5897/AJPP2013. 3487
Article Number: 4D096E551237
ISSN 1996-0816

http://www.academicjournals.org/AJPP

African Journal of Pharmacy and Pharmacology

Full Length Research Paper

Reinforcement of antibiotic activity by nanoencapsulation of ampicillin against β-lactamase producing and non-producing strains of methicillin-resistant *Staphylococcus aureus*

Jun Tonegawa, Kazuhito Ohtuka, Masuyo Nakano and Shoichi Shirotake*

Department of Pharmaco-Therapeutics, Graduate School of Medicine, Yokohama City University, Fuku-ura 3-9, Kanazawa-ku, Yokohama, 236-0004, Japan.

Received 14 February, 2013; Accepted 6 February, 2015

Ampicillin (ABPC) was encapsulated within n-butylcyanoacrylate by using dextran 70K, glucose, or the both mixtures as polymerization stabilizer, and many ABPC-nanocapsules with the various physicochemical properties were probed with the antibacterial activity against methicillin-susceptible *Staphylococcus aureus* (MSSA), methicillin-resistant *Staphylococcus aureus* (MRSA), β-lactamase producing MRSA (*blaZ* gene) and β-lactamase non-producing MRSA (no *blaZ* gene), and other germs. Morphological changes of MSSA and MRSA were assessed by scanning electron microscopy. The released ABPC was measured at various time points (1, 3, 6 or 24 h). Nanoencapsulation with ABPC resulted in an incremental increase in the antibacterial activity against MRSA penicillinase producing and non-producing strains. The nanocapsule was adhered on the cell wall of MRSA, and the morphological change was characteristically found on scanning electron microscope (SEM) image. The nanocapsulation of ABPC by n-butylcyanoacrylate was reinforced against β-lactamase producing and also non-producing strains of methicillin-resistant *Staphylococcus aureus,* and it will be a highly efficient treatment for infections caused by β-lactamase non-producing MRSA strains.

Key words: ABPC-nanocapsules; n-butylcyanoacrylate; β-lactamase non-producing MRSA.

INTRODUCTION

More than 50 years of widespread use of antibiotics has resulted in the gradual appearance of antibiotic-resistant bacteria (Leeb, 2004; Norrby et al., 2005). Methicillin-resistant *Staphylococcus aureus* (MRSA de-tection rate; ca 80%) have acquired antibiotic resistance due to the *mecA* gene that encodes alternative penicillin-binding protein (PBP 2'), resulting in the expression of an altered PBP with low affinity to methicillin (Ubukata et al., 1989).

The spread of infection by MRSA is now a serious problem. Indeed, the death toll from infection by MRSA was equal to the combined number of deaths caused by

*Corresponding author. E-mail: shirophd@med.yokohama-cu.ac.jp.

acquired immune deficiency syndrome (AIDS), lung cancer and road traffic accidents in the United States during 2005. Nowadays, MRSA is frequently isolated as multiple antibiotic-resistant pathogenic bacteria in clinical specimens, and infections of MRSA have spread from hospitals into the cities (Norrby et al., 2005). The emergence of antibiotic-resistant bacteria is worrying because the rate of discovery of novel antibacterial agents cannot keep pace. The development of new strategies to overcome the resistance mechanisms is now a global issue.

The antimicrobial-resistant mechanism of MRSA is classified into two principal types (Franciolli, 1991). One resistance mechanism is based on reduced binding affinity of β-lactam antibiotics to penicillin-binding protein (that is, from PBP to PBP2') encoded by the *mecA* gene. The second mechanism of resistance is hydrolysis of the β-lactam moiety of β-lactam antibiotics by β-lactamase, which MRSA secretes. The development of drug delivery systems (DDS) to combat the spread of antibiotic-resistant pathogens is currently attracting considerable interest (Garay-Jimenez et al., 2009; Litzinger et al., 1994; Liu et al., 2009). One such DDS comprises ampicillin enclosed by drug nano-carriers such as alkyl-cyanoacrylate. Covalent bonding of the ampicillin to *n*-butylcyanoacrylate (NBCA) occurs during production of the nanoparticles (NP). Intriguingly, this capsule was reported to protect the antibiotic from hydrolysis by β-lactamase (Fontana et al., 1998). However, β-lactamase non-producing MRSA accounts for ca 30% of clinical isolates in Japan (Yokoyama et al., 1996) and the development of a treatment for this type of MRSA remains largely unexplored.

The use of dextran70K or glucose as a polymerization stabilizer during synthesis of the nanoparticles gave the resulting preparation of a distinctive set of physico-chemical properties (Douglas et al., 1984, 1986). The present study focuses on the antimicrobial effect of various nanoparticles encapsulated with ampicillin (ABPC) on MRSA clinical isolates, which include β-lactamase producing and non-producing strains (Turos et al., 2007).

MATERIALS AND METHODS

Normal-butyl 2-cyanoacrylate (NBCA: Histoacryl®) was generously provided by B/BRAUN Aesculap AG & Co. (Tuttlingen, Germany). Dextran70000 (Dex-70K), glucose and ampicillin (ABPC) were obtained from Sigma-Aldrich (St. Louis, MO). HCl and NaOH were obtained from Wako Chemical Co. (Tokyo, Japan). All other chemicals were of analytical reagent grade and were used without further purification. Ultrapure water was used for the preparation of all solutions.

ABPC-encapsulated nanoparticles

ABPC (80 mg) was dissolved in either 0.01 M or 0.001 M HCl (20 ml). Dex70K (200 mg), glucose (1 g), or a mixture of Dex70K and glucose (Douglas et al., 1984) was added to the ABPC-hydrochloric acid solution. NBCA (0.25 ml) was added in a dropwise fashion to the ABPC-Dex70K-glucose or -Dex70K+glucose hydrochloric acid solution under stirring at room temperature. The stirring rate (650 rpm) was carefully chosen to ensure that the monomer was fully dispersed. The pH of the resulting colloidal suspension was adjusted to 7.0 by addition of 0.1 N NaOH. The suspension was then filtered through a 5 μm filter. The weight of ABPC-encapsulated nanoparticles in suspension was determined by subjecting the sample to ultracentrifugation at 100,000 *g* for 60 min. The supernatant was then discarded and the pellet of ABPC-nanocapsule freeze dried and weighed prior to re-suspension in distilled water. Each preparation was carried out in duplicate to ensure the results were reproducible. In addition, ABPC concentration of the initial supernatant was obtained using the optical density method (λ_{max} 254 nm) and defined as the amount of released ABPC that was not encapsulated in ABPC-nanocapsules. The ABPC loading rate of ABPC-nanocapsules was calculated from the encapsulated amount of ABPC divided by the additive amount: (encapsulated amount = additive ABPC - initial supernatant ABPC).

Particle size and zeta potential

The size of NBCA-NPs was assessed using a dynamic light scattering spectrophotometer Zetasizer nano (Malvern Instruments Ltd., Malvern, UK). The colloidal suspension of the NPs was diluted with deionized distilled water, and the particle size analysis was carried out at a temperature of 25°C. The zeta potential was measured on a Zetasizer Nano system (Malvern Instruments Ltd.). The measurements were performed using disposable zeta cells in accordance with a general purpose protocol at 25°C.

Bacterial strains

The standard strains were methicillin-susceptible *Staphylococcus aureus* (MSSA); ATCC6538 and JCM2874, methicillin-resistant *Staphylococcus aureus* (MRSA); JCM8703 and N315 GTC01187, *Enterococcus faecium*; JCM5804, *Escherichia coli*; ATCC8739, *Pseudomonas aeruginosa*; ATCC9027, and *Klebsiella pneumoniae*; Tf399A. Clinical isolates of MRSA (30 isolates in total) were provided by Yokohama-City University Hospital (Yokohama, Japan). The *mecA* gene was detected in all the clinical isolates. Of the 30 isolates, 18 were β-lactamase producing MRSA (*blaZ* gene 14) and 12 were β-lactamase non-producing MRSA (no *blaZ* gene).

Determination of antibacterial activity

The minimum inhibitory concentrations (MICs) of ABPC-nanocapsules were determined by the microbroth dilution method (National Committee for Clinical Laboratory Standards Institute; CLSI).

Morphological analysis of MSSA and MRSA

MSSA an MRSA were incubated in Mueller Hinton Broth (M-H Broth) with or without ABPC-nanocapsules and/or antibiotics for 24 h. After incubation, the culture suspension was filtered using Nuclepore™ Track-Etch membrane of pore size 0.1 um (Whatman Inc, Clifton, NJ). Morphological changes of MSSA and MRSA were assessed by scanning electron microscopy (type: S-800; Hitachi Corp., Tokyo, Japan), as shown in Figure 1.

Release of ABPC from the nanoparticles

One gram of dried nanoparticles encapsulated with ABPC was

Table 1. Physico-chemical property of ABPC-nanocapsules;A-D70 made by n-butyl cyanoacrylate(NBCA) and dextran 70K, A-Glucose by NBCA and glucose, A-DG by NBCA and mixture of Dex70K and glucose. Particle size: average of diameters of particles, PDI<0.131.

Polymerization pH in dil. HCl	Particle size (nm)		Zeta potential (mV)		Encapsulation Rate of ABPC (%)	
	pH2	pH3	pH2	pH3	pH2	pH3
A-D70	114	220	-20.5	-21.4	24.7	22.0
A-Glucose	99.4	190	-44.2	-49.2	25.5	22.8
A-DG	284	136	-20.4	-37.9	28.2	26.2

Table 2. MIC against ABPC sensitive Pathogensasogens; A-D70 made by n-butyl cyanoacrylate(NBCA) and dextran 70K, A-Glucose by NBCA and glucose, A-DG by NBCA and mixture of Dex70K and glucose. MIC:μg/ml upon CLSI.

Strain	*S. aureus*	*E. faecium*	*E. coli*	*P. aeruginosa*	*K. pneumoniae*
	ATCC6538	JCM5804	ATCC8739	ATCC9027	Kf399A
ABPC alone	0.06	2	2	256	64
A-D70	0.12	4	8	≥256	≥256
A-Glucose	0.12	4	4	≥256	≥256
A-DG	0.12	4	4	≥256	≥256

suspended in 100 ml of 0.9% saline. The suspension was sampled at various time points (1, 3, 6 or 24 h). The released ABPC was subsequently separated from the nanoparticles by centrifugation at 15,000 *g* for 15 min and then quantified by high performance liquid chromatography (HPLC) analysis. All experiments were performed in triplicate.

RESULTS

Physiological properties of nanocapsules with ABPC

The diameter of nanoparticles encapsulating ABPC was analyzed by the dynamic light scattering method using a Zetasizer Nano (Malvern Instruments) (Table 1). When dextran-70K or glucose was used as a polymerization stabilizer the diameter of the nanoparticles obtained in 0.01 N HCl solution (pH 2) was less than those in 0.001 N HCl (pH 3) solution. In contrast, a mixture of dextran-70K and glucose as stabilizer contributed to the production of larger nanoparticles in 0.01 N HCl solution by comparison to those generated in 0.001 N HCl solution (Table 1). Zeta potentials of nanoparticles were measured by electrophoresis using a Zetasizer Nano (Malvern Instruments). The zeta potential of nanoparticles encapsulated with ABPC using dextran-70K as stabilizer had a smaller negative charge than those prepared using glucose as stabilizer (Table I). The content of ABPC within nanoparticles in 0.01 N HCl solution was higher compared to those in 0.001 N HCl solution (Table 1).

Release of ABPC from nanocapsules

The elution profile of ABPC from the nanoparticles was biphasic with 30 to 40% of ABPC liberated after 1 to 3 h (Figure 2). The elution rate of ABPC from nanocapsules composed of dextran-70K was highest amongst the preparations analyzed in this study. The rate of release of ABPC from nanoparticles prepared in the presence of a mixture of dextran-70K and glucose was greater than those prepared in the presence of glucose only. The release profile of ABPC from nanocapsules made in the presence of glucose only was like monophasic that is, gradual release of ABPC from the capsule.

Antibacterial activity of the ABPC-nanoparticles

Antibacterial activity as MIC was examined against several common pathogenic bacteria, *S. aureus*, *E. faecium*, *E. coli*, *P. aeruginosa* and *K. pneumonia,* as standard strains (Table 2). The antibacterial activity of the ABPC nanocapsules against *S. aureus* and *E. faecium* decreased to approximately 1/2 that of ABPC alone. Moreover, the antibacterial activity against *E. coli* decreased from 1/2 to 1/4 that of ABPC alone. *P. aeruginosa* and *K. pneumoniae* were resistant to both ABPC and ABPC-nanocapsules. By contrast, nanoencapsulation with ABPC resulted in an incremental increase in the antibacterial activity against MRSA. Moreover, the antibacterial activity of ABPC nanocapsules obtained in 0.01 HCl increased by 4 to 8 fold compared with ABPC alone (Table 3). The antimicrobial activity of ABPC nanocapsules against MRSA-*blaZ*(+) strains, which produce penicillinase, was compared with that against MRSA-*blaZ*(-) strains, which are penicillinase non-producers (Table 3). The MRSA-*blaZ*(+) strain was much more resistant to ABPC alone than the MRSA-*blaZ*(-) strain. However, the antimicrobial activity of ABPC nanocapsules against the MRSA-*blaZ*(+) and

Table 3. MIC against MRSA (producing penicillinase); A-D70 made by n-butyl cyanoacrylate(NBCA) and dextran 70K, A-Glucose by NBCA and glucose, A-DG by NBCA and mixture of Dex70K and glucose. MIC:μg/ml upon CLSI.

Polymerization pH in dil. HCl	MRSA: (N315 strain)		MRSA: (JCM8703 strain)	
	pH2	pH3	pH2	pH3
A-D70	8	16	16	16
A-Glucose	16	16	32	32
A-DG	8	16	8	8
ABPC alone	32		64	

MRSA-*blaZ*(-) strains was stronger by 8- and 4-fold, respectively, compared with ABPC alone.

Antibacterial activity of the ABPC nanoparticles to MRSA-clinical isolates

The antibacterial activity of ABPC nanocapsules was compared to ABPC, tetracycline (TC), clarithromycin (CAM), and vancomycin (VCM) alone (Table 4). Although many of the MRSA strains displayed multiple antibiotic drug resistance and were resistant to both TC and CAM, they were all sensitive to the ABPC-nanocapsules, as VCM. However, methicillin sensitive *S. aureus* were sensitive to ABPC, TC, CAM and VCM.

DISCUSSION

In this study, the antibacterial activity of the ABPC-nanocapsules against MRSA pathogens was evaluated based on the physiochemical properties of each of the nanocapsules *in vitro*. The antibacterial activity of the ABPC-nanocapsules against several common ABPC sensitive pathogens was assessed. Our findings show that the antibacterial activity of ABPC-nanocapsules was 1/2 that of ABPC alone against *S. aureus* and *E. faecium* (Table 2). Moreover, the antibacterial activity of ABPC-nanocapsules was 1/4 that of ABPC alone against *E. coli* (Table 2). The ABPC-nanocapsules had no antibacterial activity against *P. aeruginosa* and *K. pneumonia*, which were resistant to ABPC. The lower level of activity of the ABPC-nanocapsules towards Gram-negative bacteria by comparison to Gram-positive bacteria is thought to result from the structure of their outer cell wall. Specifically, the presence of lipopolysaccharide (LPS) in the outer cell wall in the Gram-negative bacteria is believed to act as an effective barrier to prevent uptake of the antibiotic into the cell (Snyder and McIntosh, 2000). LPS is absent in Gram-positive bacteria resulting in higher antimicrobial activity of ABPC-nanocapsules.

The antibacterial activity of ABPC-nanocapsules against MRSA was found to be more potent than ABPC alone (Table 3). The mutation of PBP to PBP2' in MRSA decreases the affinity of this protein for β-lactam antibiotics (Hartman and Tomasz, 1981; Piddock et al., 1992). The binding properties of nanoparticles are strongly influenced by the zeta potential on their surface (Hu et al., 2002; McCarron et al., 1999). The integrated surface structure of the ABPC-nanocapsules is closely related to their enhanced affinity for PBP2' rather than PBP. Another antibiotic resistance mechanism found in MRSA is the production of β-lactamase. The covalent binding of ABPC to ethylcyanoacrylate nanoparticles has been reported (Fontana, 1998) to prevent the hydrolysis of β-lactam antibiotics by β-lactamase. The MIC50 and MIC90 of ABPC-nanocapsules against clinical isolates of MRSA were lower than those of ABPC alone, as shown in Table 4. For penicillinase producing clinical isolates, the ABPC-nanocapsules gave much greater antimicrobial activity over ABPC alone. The effect of encapsulating ABPC within nanoparticles to protect against hydrolysis by β-lactamase was first assessed in this study (Tables 3 and 4). Furthermore, the MIC50 and MIC90 of ABPC-nanocapsules against penicillinase non-producing clinical isolates were also lower than those of ABPC alone. These results show that the antibacterial activity of ABPC within nanoparticles is reinforced against MRSA penicillinase producing and non-producing strains.

Given that the antibacterial activity of ABPC is enhanced by nanoencapsulation against β-lactamase producing and non-producing strains, the improved antimicrobial activity does not solely arise from avoiding the effect of β-lactamase. Thus, the morphological changes in MRSA caused by ABPC-nanocapsules were different from those induced by ABPC alone (Figure 1). It is likely that binding of ABPC-nanocapsules to the cell wall will result in a release of ABPC at high concentration close to the adherence point. The release of ABPC from ABPC-nanocapsules was categorized as monophasic or biphasic depending on the polymerization stabilizer used to prepare the nanocapsules (Figure 2). For example, ABPC is released in a biphasic manner (i.e. ~40% ABPC after 4 h) from the ABPC encapsulation by ethylcyanoacrylate (Fontana, 1998).

In this study, 65% ABPC was released from ABPC-nanocapsules after 24 h. The surface property of

Table 4. MIC of ABPC, TC, CAM, VCM, and ABPC-nanocapsules against MSSA and MRSA (producing penicillinase strains upon *bla*Z gene, and non-producing penicillinase strains).

Strain	*blaZ*	ABPC	TC	CAM	VCM	ABPC-nanocapsules
MSSA 6538	-	≤0.06	0.125	≤0.125	1	0.125
2874	-	2	0.5	0.25	1	4
MRSA N315	+	32	0.125	≥128	1	16
8703	+	64	256	≥128	2	16
MRSA clinical isolates						
1423	-	16	0.5	0.5	1	2
1846	-	8	64	≥256	1	4
1801	-	16	64	≥256	1	8
1858	-	16	64	≥256	1	2
2022	-	16	64	256	1	8
2046	-	16	64	256	0.5	2
2137	-	16	0.5	256	0.5	4
2232	-	8	64	256	0.5	4
2790	-	8	64	256	1	2
3077	-	8	64	256	1	2
3223	-	8	64	256	1	2
3811	-	8	32	≥256	1	2
1447	+	32	32	≥256	0.5	4
1739	+	128	64	≥256	1	4
1847	+	64	0.5	≥256	1	4
1870	+	64	64	≥256	1	4
2005	+	64	8	128	0.5	16
2107	+	128	64	≥256	0.5	4
2370	+	128	2	128	0.5	8
2526	+	64	0.5	128	0.5	8
2836	+	16	64	256	1	4
2928	+	32	64	256	1	8
3137	+	16	16	256	0.5	4
3200	+	32	0.5	256	0.5	4
3334	+	16	64	≥256	0.5	4
3351	+	8	0.5	0.5	0.5	4
3428	+	32	64	≥256	1	4
3785	+	16	64	≥256	1	4
4147	+	64	64	≥256	1	4

Resistance upon CLSI: ABPC ≥ 0.5 µg/ml, TC ≥ 16 µg/ml, CAM ≥ 8 µg/ml, VCM ≥ 32 µg/ml. MIC50 against MRSA *blaZ*(+) strains: 4 µg/ml, MIC90: 8 µg/ml. MIC50 against MRSA *blaZ*(-) strains: 2 µg/ml, MIC90: 8 µg/ml.

the nanoparticles differ depending on the type of cyanoacrylate derivative and polymerization initiator (Table 1) used in their preparation. In addition, the surface property affects the release rate of ABPC (Figure 2). The antibacterial activity of ABPC-nanocapsules can be deduced from the following equation:

(Antimicrobial activity of ABPC-nanocapsules) = (activity of released ABPC) + (activity(X) on binding nanocapsules)

The MIC value of ABPC alone was put into the (Antimicrobial activity) part of the equation. The concentration of released ABPC was put into (activity of released ABPC), and the (activity(X) on binding nanocapsules) was calculated from the conjugation index.

Table 5. The antimicrobial activity (X) by binding ABPC-nanocapsules against MSSA and MRSA (producing penicillinase strains upon *bla*Z gene, and non-producing penicillinase strains).

Staphylococcus aureus	Activity(X) by binding ABPC-nanocapsules					
	Nanocapsules from Dex-70K		Nanocapsules from glucose		Nanocapsules from Dex-70K and glucose	
MSSA	-0.43	<0	-0.01	<0	-0.05	<0
ATCC6538	-4.22	<0	-0.04	<0	-1.38	<0
JCM2874						
MRSA (*bla* Z+strain)	+28.77	>0	+23.86	>0	+28.66	>0
N315	+57.54	>0	+48.07	>0	+60.66	>0
JCM8703						
Clinically isolated MRSA (*bla* Z-strain)	+9.54	>0	+7.86	>0	+9.36	>0
1801	+9.54	>0	+7.86	>0	+9.36	>0
2022						
Clinically isolated MRSA (*bla* Z+strain)	+57.54	>0	+48.07	>0	+60.66	>0
2005	+57.54	>0	+48.07	>0	+57.36	>0
2526						

X>0: the decrement of antibacterial activity. X<0: the increment of antibacterial activity.

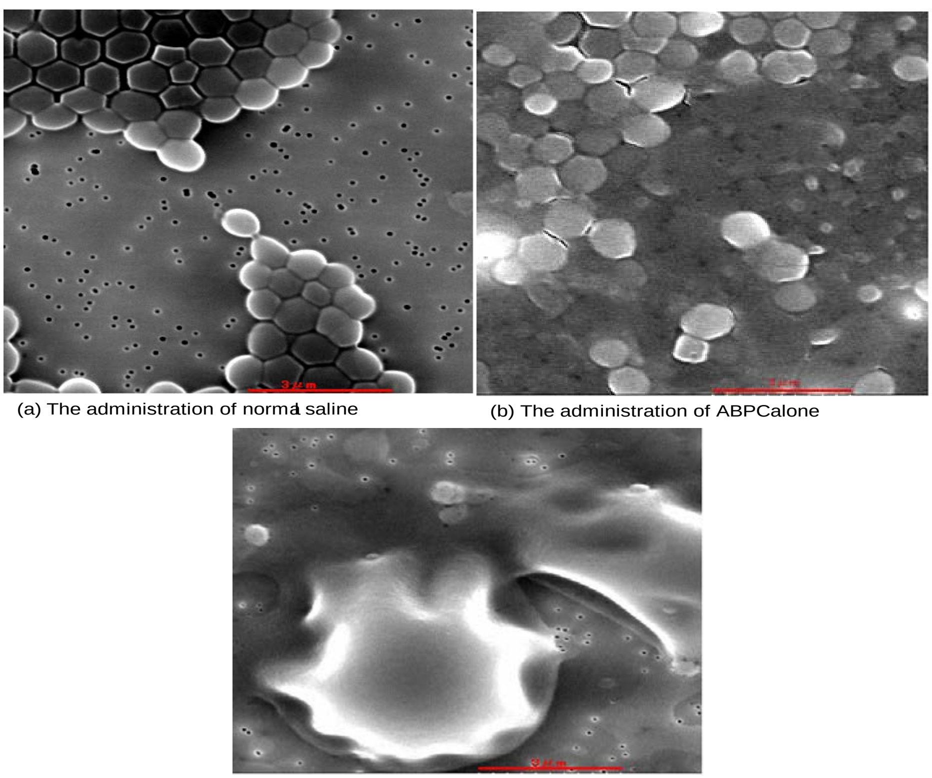

(a) The administration of normal saline

(b) The administration of ABPCalone

(c) The administration of ABPG nanocapsules

Figure 1. The morphological changes of MRSA(N315) caused by ABPC-nanocapsules after 12 h (on SEM image× 10,000). Black spots are filter holes (approx. 100nm). Nanocapsules were binding on surface of MRSA.

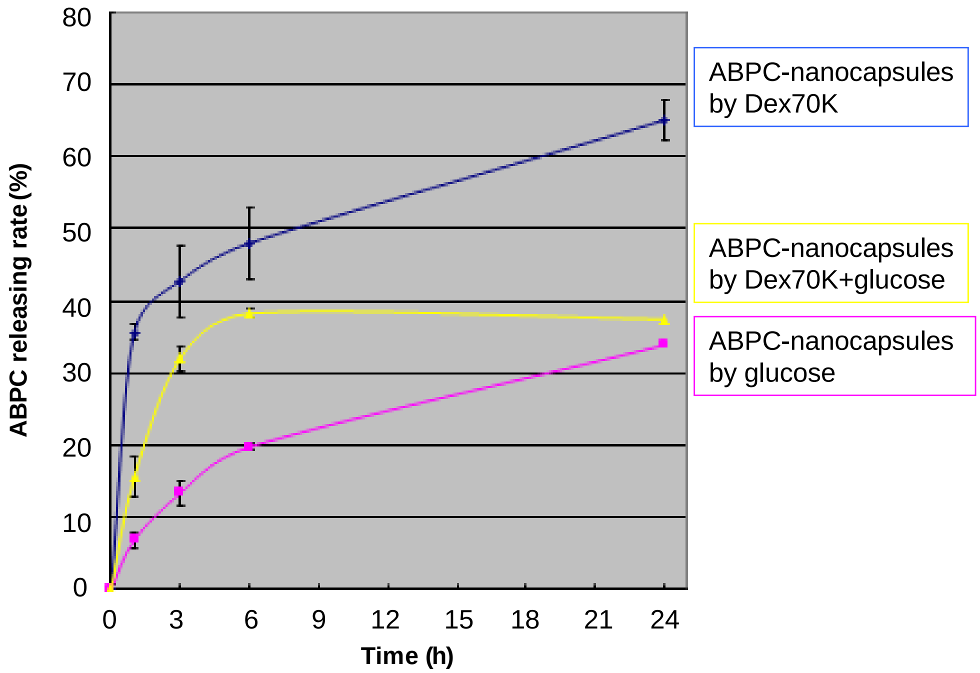

Figure 2. ABPC releasing profiles from ABPC-nanocapsules made by Dextran 70K, by Dextran 70K+glucose, or by glucose.

When the "activity of a nanoparticle" was set to X from this formula, X ≥ 0 shows antimicrobial activation reinforcement, whereas X ≤ 0 shows an antimicrobial activity attenuation effect (Table 5).

We conclude that the nanocapsulation of ABPC by n-butylcyanoacrylate was reinforced against β-lactamase producing and also non-producing strains of methicillin-resistant *S. aureus,* and that it will be a highly efficient treatment for caused by β-lactamase non-producing MRSA strains.

ACKNOWLEDGEMENTS

The clinical isolated MRSA strains were kindly provided by T. Mituda, Yokohama City University Hospital (Japan). The authors thank N. Sasatu, Tokyo Pharmacy University (Japan) for valuable comments, and N. Hotoki for technical assistance. This work was supported by Grants-Aid for Scientific Research (No. 20659069 to S.S.) from the Ministry of Education, Culture, Sports, Science and Technology of Japan.

REFERENCES

Douglas SJ, Illum L, Davis SS (1984). Particle size and size distribution of poly(butyl-2-cyanoacrylate) nanoparticles: I. Influence of physicochemical factors. J. Colloid Interface Sci. 101(1):149-58.

Douglas SJ, Illum L, Davis SS (1986). Poly (butyl-2-cyanoacrylate) nanoparticles with differing surface charges. J. Control Release 15-23.

Fontana G, Pitarresi G, Tomarchio V, Carlisi B, San Biagio PL (1998). Preparation, characterization and in vitro antimicrobial activity of ampicillin-loaded polyethylcyanoacrylate nanoparticles. Biomaterials 19(11-12):1009-17.

Franciolli M, Bille J, Glauser MP, Moreillon P (1991). Beta-lactam resistance mechanisms of methicillin-resistant *Staphylococcus aureus*. J. Infect. Dis. 163(3):514-23.

Garay-Jimenez JC, Gergeres D, Young A, Lim DV, Turos E (2009). Physical properties and biological activity of poly(butyl acrylate-styrene) nanoparticle emulsions prepared with conventional and polymerizable surfactants. Nanomedicine 5(4):443-51.

Hartman B, Tomasz A (1981). Altered penicillin-binding proteins in methicillin-resistant strains of *Staphylococcus aureus*. Antimicrob. Agents Chemother. 19(5):726-35.

Hu Y, Jiang X, Ding Y, Ge H, Yuan Y, Yang C (2002). Synthesis and characterization of chitosan-poly(acrylic acid) nanoparticles. Biomaterials 23(15):3193-201.

Leeb M (2004) Antibiotics: a shot in the arm, Nature 431:892 -893.

Litzinger DC, Buiting AM, van Rooijen N, Huang L (1994). Effect of liposome size on the circulation time and intraorgan distribution of amphipathic poly(ethylene glycol)-containing liposomes. Biochim. Biophys. Acta 1190(1):99-107.

Liu PF, Lo CW, Chen CH, Hsieh MF, Huang CM (2009). Use of nanoparticles as therapy for methicillin-resistant *Staphylococcus aureus* Infections. Curr. Drug Metab. 10(8):875-84.

McCarron PA, Woolfson AD, Keating SM (1999). Response surface methodology as a predictive tool for determining the effects of preparation conditions on the physicochemical properties of poly(isobutylcyanoacrylate) nanoparticles. Int J Pharm 193(1):37-47.

Norrby SR, Nord CE, Finch R (2005). Lack of development of new antimicrobial drugs: a potential serious threat to public health, Lancet Infect. Dis. 5:115-119.

Piddock LJ, Traynor EA, Griggs DJ (1992). Activity of cefpirome combined with beta-lactamase inhibitors and affinity for the penicillin-binding proteins of methicillin-resistant *Staphylococcus aureus*. Eur. J. Clin. Microbiol. Infect. Dis. 11(4): 364-71

Snyder DS, McIntosh TJ (2000). The lipopolysaccharide barrier: correlation of antibiotic susceptibility with antibiotic permeability and fluorescent probe binding kinetics. Biochemistry 39(38):11777-87.

Turos E, Reddy GS, Greenhalgh K, Ramaraju P, Abeylath SC, Jang S, Dickey S, Lim DV (2007). Penicillin-bound polyacrylate nanoparticles: restoring the activity of beta-lactam antibiotics against MRSA. Bioorg. Med. Chem. Lett. 17(12): 3468-72.

Ubukata K, Nonoguchi R, Matsuhashi M, Konno M (1989). Expression and inducibility in *Staphylococcus aureus* of the *mecA* gene, which encodes a methicillin-resistant *S. aureus*-specific penicillin-binding protein. J. Bacteriol. 171(5): 2882-5.

Yokoyama T, Honda J, Kawayama T, Kajimura K, Oizumi K (1996). Increased incidence of beta-lactamase-plasmid negative, high level methicillin-resistant *Staphylococcus aureus* (MRSA). Kurume Med. J. 43(3):199-206.

academicJournals

Vol. 9(7), pp. 198-204, 22 February, 2015
DOI: 10.5897/AJPP2014. 4019
Article Number: xxxxx
ISSN 1996-0816

http://www.academicjournals.org/AJPP

African Journal of Pharmacy and Pharmacology

Full Length Research Paper

Reversal of phenytoin induced hepatotoxicity by alpha lipoic acid in rats

Ganesan Rajalakshmi Saraswathy[1]*, Eswaran Maheswari[2], Thakur Santhrani[3] and Jayaraman Anbu[1]

[1]Department of Pharmacology, Faculty of Pharmacy, M.S. Ramaiah University of Applied Sciences, Bangalore, Karnataka, India.
[2]Department of Pharmacy Practice, Faculty of Pharmacy, M.S. Ramaiah University of Applied Sciences, Bangalore, Karnataka, India.
[3]Division of Pharmacology, Institute of Pharmaceutical Technology, Sri Padmavathi Mahila Visvavidyalayam (Women's University), Tirupati, Andhra Pradesh, India.

Received 20 January, 2014; Accepted 26 January, 2015

The present research task is aimed at evaluating the influence of alpha lipoic acid (ALA) against phenytoin induced hepatotoxicity. The rats were divided into five groups of six animals each. Group 1 received 0.2% carboxy methyl cellulose (CMC, p.o), group 2 received 20 mg/kg phenytoin (p.o), groups 3, 4 and 5 received 50, 100 and 200 mg/kg (p.o) of ALA in 0.2% CMC, respectively 1 h prior to phenytoin for 45 days. On the 45th day, blood samples were collected and subjected to analysis of liver function test. Animals were sacrificed, antioxidant status and lipid peroxidation were estimated in the liver samples along with histopathological investigations. Phenytoin treatment was observed to induce liver injury, which was apparent from increased serum transaminases, alkaline phosphatase (ALP) and bilirubin in blood, and lipid peroxidation in liver. Phenytoin decreased the levels of albumin, total protein, and endogenous antioxidants along with reduction in body weight. Histopathological investigation revealed phenytoin induced periportal congestion and hepatic necrosis. ALA (100 and 200 mg/kg) significantly ($P < 0.001$) reduced the phenytoin elevated serum enzymes, ALP, bilirubin, lipid peroxidation, liver weight and significantly increased the levels of albumin, total protein, antioxidant levels and body weight reduced by phenytoin. ALA effectively reversed the phenytoin induced histopathological changes. ALA was found to be effective against phenytoin induced hepatotoxicity.

Key words: Phenytoin, alpha lipoic acid (ALA), hepatotoxicity, oxidative stress, antiepileptics, antioxidant.

INTRODUCTION

Aromatic antiepileptic drug (AAED) therapy has been expanded to a broad spectrum of psychiatric and neurological disorders. However, the clinical use of these drugs is limited by several adverse effects, mainly hepatotoxicity. Metabolites of AAEDs are proven to be responsible for the occurrence of oxidative stress resulting in hepatic damage (Santos et al., 2008). Reactive metabolites from AAED lead to direct cytotoxicity and liver cell necrosis

*Corresponding author. E-mail: saraswathypradish@gmail.com. Tel: 08123230400. Fax: 080-23607488.

and liver cell necrosis (Björnsson, 2008).

Phenytoin is one of the most commonly used AAEDs in the treatment of generalized as well as secondarily generalized tonic clonic seizures (Walker, 2005). Phenytoin induced hepatotoxicity is one of the most recurrently reported adverse effects induced by the drug (Walia et al., 2004). 10 to 38% of the patients were observed to show fatal outcome subsequent to phenytoin induced liver damage (Dreifuss and Langer, 1987). It was observed that there was an increase in hepatic enzymes such as transaminases, lactic dehydrogenase, alkaline phosphatase and gamma glutamyl transferase along with serum bilirubin in patients receiving phenytoin (Aldenhovel, 1988; Kazamatsuri, 1970; Smythe and Umstead, 1989). The drug also brought about morphologic and pathologic abnormalities such as primary hepatocellular degeneration and necrosis (Harden, 2000). 95% of phenytoin is metabolized in the liver and less than 5% is eliminated unchanged in the urine (Bajpai et al., 1996). AAED induced hepatotoxicity was considered to be due to defect in epoxide hydrolase detoxification process resulting in accumulation of arene oxides (Bavdekar et al., 2004; Kass, 2006). It was reported that the metabolites of phenytoin produced severe oxidative stress on the rat hepatic mitochondria resulting in mitochondrial dysfunction (Santos et al., 2008). The aforementioned studies suggested oxidative stress mediated via reactive oxygen species to be one of the contributing factors of phenytoin induced liver damage. Our previous study also confirmed that phenytoin induced liver damage had an etiological background of oxidative stress (Saraswathy et al., 2010).

Alpha lipoic acid (ALA) is a powerful antioxidant often termed as "universal antioxidant" as it neutralizes free radicals in both aqueous and lipid media of cells. ALA functions as both fat and water soluble antioxidant that easily crosses cell membranes, thereby it confers free radical protection to both interior and exterior cellular structures. The antioxidant capacity of ALA is retained in both its reduced and oxidised forms (Packer et al., 1995). ALA was used to treat liver poisoning induced by alcohol, mushroom and heavy metals. The antioxidant abilities of ALA and its role in glutathione recycling have encouraged its use in liver damage. ALA was also reported to exhibit a very significant hepatoprotective effect against chloroquine induced hepatotoxicity than silymarin, a reference drug (Pari and Murugavel, 2004).

As phenytoin induced hepatic damage was induced by oxidative stress; the present study was undertaken to investigate the intervention of an antioxidant ALA on phenytoin induced hepatotoxicity.

MATERIALS AND METHODS

Animals

Adult male albino rats weighing 150 to 200 g were selected and housed in propylene cages at room temperature (25 ± 3°C). All through the study, they were fed *ad libitum* on standard pellet feed and freely provided drinking water. The study protocol was approved by the Institutional Animal Ethical Committee of M.S. Ramaiah College of Pharmacy, Reference number 220/abc/CPCSEA.

Study protocol

The rats were divided into five groups of six animals each. Group 1 served as control and received 0.2% carboxy methyl cellulose (CMC) (orally) for 45 days. Group 2 received 20 mg/kg phenytoin (orally) for 45 days. Groups 3, 4, and 5 received 50, 100 and 200 mg/kg (orally) of ALA in 0.2% CMC, respectively 1 h prior to administration of 20 mg/kg phenytoin for 45 days. On the 45th day of the drug administration, the animals were anaesthetized under ether anaesthesia and the blood samples were collected from retro orbital plexus for estimation of serum biochemical parameters such as total protein (Gomall et al., 1949; Lowry et al., 1951), albumin (Doumasa et al., 1971), serum glutamate oxaloacetate transaminase (SGOT) (Gella et al., 1985), serum glutamate pyruvate transaminase (SGPT) (Gella et al., 1985), alkaline phosphatase (ALP) (Rosalki et al., 1993) and total bilirubin (Pearlman and Lee, 1974) were analyzed by enzymatic kit (AGAPPE, India) and an autoanalyser (Chemistry Analyser (CA 2005), B4B Diagnostic Division, China). Animals were then sacrificed; liver tissues were dissected out and were rinsed with cold phosphate buffer (PB, 100 mM, pH 7.4), weighed, sliced for histopathological studies and stored at -40°C. The stored tissues were homogenized and the homogenate was centrifuged at 10,000 × g for 10 min at 4°C. The supernatant was stored at -40°C for estimation of lipid peroxidation (to measure the extent of oxidative stress) by malondialdehyde method (Chatterjee and Sil, 2006) and antioxidants such as superoxide dismutase (SOD) by pyrogallol auto oxidation method (Marklund and Marklund, 1974), catalase (Beer and Sizer, 1952) by hydrogen peroxide method and reduced glutathione (GSH) by Ellman's method (Sedlak and Lindsay, 1968). The levels of endogenous antioxidants were estimated only in liver homogenates in order to assess the extent of liver damage.

Histopathological studies

Rats were anesthetized under ether anesthesia and sacrificed. The liver was fixed in 4% paraformaldehyde overnight. Block was prepared in block preparation unit (Shandon Histocenter-2) and sections (10 µm) were cut with the help of a microtome (Leica RM 2255, Lab India) and picked up on poly-l-lysine coated slides and were stained with hematoxylin and eosin (Li et al., 1998).

Statistical analysis

The results were expressed as mean ± standard error of mean (SEM; n=6). The statistical analysis was performed by means of analysis of variance (ANOVA) followed by Tukey-Kramer's Multiple Comparison Test. p value < 0.05 was considered as statistically significant. Data were processed with Graphpad Instat Software.

RESULTS

Effect of ALA on phenytoin induced alterations in hepatic parameters

Administration of phenytoin 20 mg/kg for a period of 45 days significantly increased the levels of SGOT, SGPT, total bilirubin and ALP along with a significant decrease

Table 1. Effect of ALA on phenytoin induced alterations in liver parameters.

Parameter	Control	Phenytoin (20 mg/kg)	PHT+ALA 50 mg/kg	PHT+ALA 100 mg/kg	PHT+ALA 200 mg/kg
SGOT (IU/L)	254.5±4.5+++	376.3±5.45***	324.8±3.8***+++	299.6±6.4***+++	263±2.769+++
SGPT (IU/L)	67.68±1.6+++	91.75±0.9***	75.3±0.65***+++	72±0.847*+++	69.27±0.77+++
TBL (mg/dl)	1.29±0.07+++	2.45±0.12***	2.2 ± 0.122***	1.723 ± 0.5**+++	1.39±0.065+++
ALP (IU/L)	147.6±4.5+++	250.1±3.28***	210.6±4.8***+++	180.1±6.0***+++	150.5±3.63+++
ALB (g/dl)	4.47±0.22+++	3.15±0.072***	3.52±0.185***	3.98±0.15++	4.34±0.149+++
TP (g/dl)	7.82±0.83+++	5.56±0.083***	6.2±0.285***+	6.93±0.128**+++	7.5±0.056+++
LLP (nmol/g wet tissue)	32.8±0.47+++	119.2±0.67***	91.75±0.9***+++	75.68±1.1***+++	52.05±1.3***+++
SOD (Superoxide anion reduced/mg protein/min)	5.8±0.036+++	2.12±0.046***	2.7±0.049***+++	3.48±0.1***+++	4.4±0.074***+++
Catalase (μmol H_2O_2 degraded/mg protein/min)	58.9±0.83+++	40.09±0.45***	42.9±0.45***+++	46.3±0.61***+++	51.4±0.70***+++
GSH (mg/dl)	17.5±0.22+++	11.48±0.43***	12.58±0.24***+	13.33±0.24***++	14.8±0.23***+++

Values are expressed as mean± SEM of 6 animals. ***p < 0.001 versus control group, **p < 0.01 versus control group, *p < 0.05 versus control group; $^{+++}$p < 0.001 versus Phenytoin group, $^{++}$p < 0.01 Phenytoin group, $^{+}$p < 0.05 Phenytoin group.

in the levels of albumin and total protein. ALA (50 and 100 mg/kg) significantly (p < 0.001) decreased the elevated SGOT levels when compared with phenytoin treated animals, but the values did not reach that of normal. ALA at its higher dose (200 mg/kg) dropped off the levels of SGOT near to that of normal control animals. ALA (50 and 100 mg/kg) significantly (p < 0.001) decreased the levels of SGPT when compared with phenytoin treated animals, but the values did not reach that of the normal. ALA (200 mg/kg) decreased the levels of SGPT near to that of normal control. ALA at 50 mg/kg showed no significant decrease in the levels of total bilirubin elevated by phenytoin, whereas at 100 mg/kg ALA significantly (p < 0.001) reduced the levels of total bilirubin and at 200 mg/kg the values were brought near that of normal values. ALA at the dose of 50 and 100 mg/kg significantly (p < 0.001) brought down the levels of ALP but not closer to the normal values, whereas the antioxidant at its higher dose (200 mg/kg) decreased the levels of ALP near to that of normal control. ALA at the dose of 50 mg/kg showed no significant increase in the levels of albumin, whereas at 100 and 200 mg/kg ALA augmented the levels of albumin in a dose dependent fashion and at the dose of 200 mg/kg, a significant (p < 0.001) increase in the levels of albumin near to that of normal control was observed. ALA at the dose of 50 mg/kg slightly increased the levels of total protein (p < 0.05), whereas at 100 and 200 mg/kg, significantly (p < 0.001) augmented the levels of total protein (Table 1).

Effect of ALA on phenytoin enhanced liver lipid peroxidation

Administration of phenytoin 20 mg/kg for a period of 45 days significantly increased the lipid peroxide contents in liver. ALA at all the three doses (50, 100 and 200 mg/kg) significantly (p < 0.001) reduced the liver lipid peroxidation in a dose dependent manner but the values did not reach the normal (Table 1).

Effect of ALA on phenytoin depleted endogenous enzymatic and non enzymatic antioxidants

Administration of phenytoin 20 mg/kg for a period of 45 days significantly decreased the endogenous enzymatic antioxidants such as SOD as well as catalase and non enzymatic antioxidant GSH in liver. ALA at all the three doses (50, 100 and 200 mg/kg) significantly increased the endogenous antioxidant levels decreased by phenytoin in a dose dependent manner but the values did not reach the normal (Table 1).

Effect of antioxidants on phenytoin induced alterations in body weight, absolute and relative liver weight

At the end of 45 days of treatment with phenytoin, there was a statistically significant decrease in body weight and an increase in the absolute and relative liver weights when compared with the

Table 2. Effect of phenytoin and phenytoin + ALA on body weight, absolute and relative liver weight.

Group	Body weight (g)			Absolute liver weight (g)	Relative liver weight (g)
	Initial	Final	Percent change		
Control	225	268.3±2.1	$19.2±0.93^{+++}$	$12.7±0.081^{+++}$	$4.7±0.05^{+++}$
Phenytoin	228.3±4.4	201.6±1.0	-11.3±0.6***	14.6±0.056***	7.2±0.06***
Phenytoin+ALA 50 mg/kg	222.5±2.14	211.6±2.4	$-4.8±1.0^{***,+++}$	$13.5±0.09^{***,+++}$	$6.4±0.07^{***,+++}$
Phenytoin+ALA100 mg/kg	221.66±3.3	216.6±3.0	$-2.1±0.9^{***,+++}$	$13.01±0.09^{*,+++}$	$5.9±0.11^{***,+++}$
Phenytoin+ALA 200 mg/kg	229.16±1.5	225±1.29	$-1.8±0.7^{***,+++}$	$12.78±0.11^{+++}$	$5.7±0.05^{***,+++}$

Values are expressed as mean± SEM of 6 animals. ***p < 0.001 versus control group, **p < 0.01 versus control group, *p < 0.05 versus control group; $^{+++}$p < 0.001 versus Phenytoin group, $^{++}$p < 0.01 Phenytoin group, $^{+}$p < 0.05 Phenytoin group.

control group. ALA at the dose of 50 mg/kg showed no significant difference in body weight or absolute and relative liver weight. ALA at its higher doses (100 and 200 mg/kg) reversed the phenytoin induced weight loss and decreased the absolute and relative liver weights significantly when compared with phenytoin group (Table 2).

Effect of ALA on phenytoin induced alterations in liver histopathology

On histopathological examination, the livers of the control group revealed normal hepatic architecture (Figure 1A). Figure 1B and C represented the phenytoin group and showed severe congestion, periportal inflammation revealing centrilobular congestion, fatty degeneration and hepatocellular necrosis. Phenytoin + ALA (50 mg/kg) treated group showed mild hepatic necrosis and mild congestion in liver (Figure 1D), ALA (100 mg/kg) showed mild hepatic necrosis (Figure 1E). Thus ALA (50 and 100 mg/kg) decreased the extent of hepatic damage induced by phenytoin. ALA (200 mg/kg) treated group showed normal hepatic parenchyma (Figure 1F).

DISCUSSION

AAED induced hepatotoxicity correlated to the accumulation of arene oxides metabolites of phenytoin which are reported to be involved in the pathogenesis of hepatotoxicity (Bavdekar et al., 2004). Santos et al. (2008) elucidated the mechanism of phenytoin induced hepatic damage and revealed that oxidative stress to be one of the potential mechanisms responsible for phenytoin associated hepatotoxicity.

Oxidative stress induced by the metabolites of phenytoin have been suggested to be formed after its biotransformation both in humans and in rats (Bavdekar et al., 2004; Shear and Spielberg, 1988; Roy and Snodgrass, 1988; George and Farrell, 1994; Madden et al., 1996; Kalapos, 2002; Zaccara et al., 2007). Santos et al. (2008) demonstrated AAED induced depletion of the mitochondrial antioxidant defense in rat liver. These findings might explain the potential role of mitochondrial toxicity and oxidative stress in the hepatotoxicity in associated with AAED therapy. Also, in the present study, phenytoin increased lipid peroxidation and depleted the endogenous antioxidants such as SOD, catalase and GSH in liver revealing massive oxidative stress in liver.

SGOT, SGPT, ALP and bilirubin are markers used to assess hepatic damage (Sallie et al., 1991; Ncibi et al., 2008; Gokcimen et al., 2007; Eraslan et al., 2009). A low serum albumin indicates poor liver function, reductions in albumin levels shows the presence of underlying liver disease (Kalender et al., 2010). In this investigation phenytoin treated rats showed a significant increase in the levels of SGOT, SGPT, bilirubin and ALP and decrease in the levels of albumin and total protein which indicates the hepatotoxic nature of the drug phenytoin. Phenytoin was observed to alter protein and free amino acid metabolism and their synthesis in the liver. The body weight of phenytoin treated rats was decreased whereas the relative liver weight was increased.

Phenytoin exhibited periportal inflammation, hemorrhage, sinusoidal congestion and hepatic necrosis in rat liver which was revealed by histopathological investigation. These changes were online with the changes in various biochemical parameters investigated and liver damage was considered to arise from the toxic effects of phenytoin mediated via oxidative stress.

ALA was used to treat liver poisoning induced by alcohol, mushroom and heavy metals. The antioxidant abilities of ALA and its role in glutathione recycling have encouraged its use in liver damage. ALA (100 mg/kg/day) was reported to exhibit a significant hepatoprotective against chloroquine induced hepatotoxicity. It was also observed that ALA had a better protective effect than silymarin, a reference drug (Pari and Murugavel, 2004). Hesham (2007) elucidated the effects of ALA against tamoxifen (TAM) induced liver damage, oxidative stress and DNA fragmentation. ALA was described to scavenge free radicals, prevent DNA fragmentation, reduce liver injury and protect oxidative stress induced by TAM intoxication. The study suggested the use of ALA in the prophylactic treatment of TAM induced liver injury than its

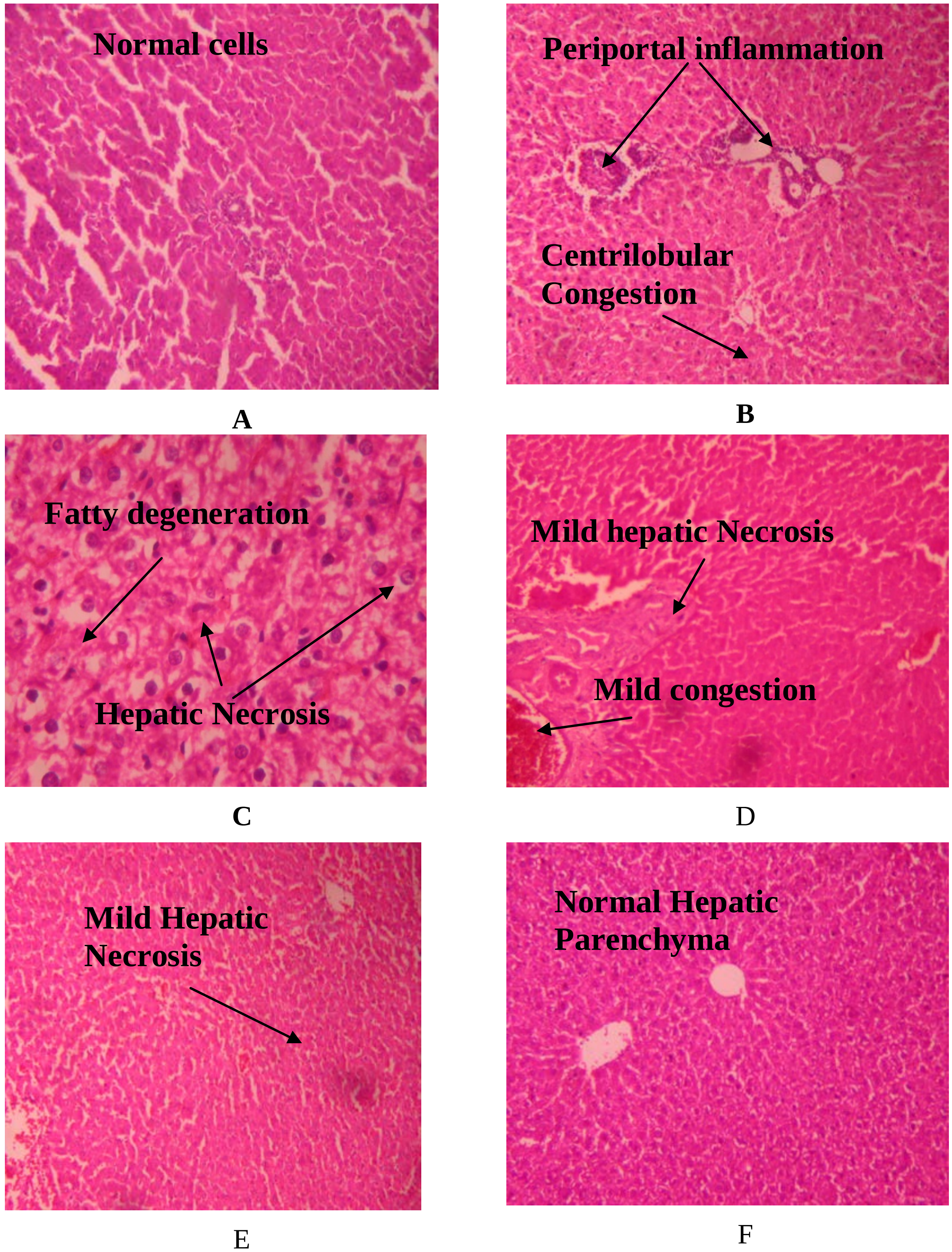

Figure 1. Micrograph showing effect of phenytoin and ALA on hepatocytes. (A) Control showing normal hepatocytes. (B) Phenytoin treated group showing severe congestion and periportal inflammation revealing centrilobular congestion. (C) Phenytoin treated group showing fatty degeneration and hepatocellular necrosis. (D) Phenytoin + 50 mg/kg ALA treated group showed mild congestion and hepatic necrosis. (E) Phenytoin + 100 mg/kg ALA treated group showed mild hepatic necrosis. (F) Phenytoin + 200 mg/kg ALA treated group showed normal hepatic parenchyma.

use as curative agent (post-TAM administration) (Hesham, 2007). The effects of ALA and its reduced form dihydrolipoic acid (DHLA) was studied by Foo et al. (2011) against thioacetamide (TAA) induced liver fibrosis in rats and the possible underlying mechanisms in hepatic stellate cells *in vitro*. It was found that co-administration of ALA to rats chronically treated with TAA inhibited the development of liver cirrhosis, as indicated by reductions in cirrhosis incidence, hepatic fibrosis and AST, ALT activities. ALA exhibited beneficial role in the treatment of chronic liver diseases caused by ongoing hepatic damage (Foo et al., 2011). Liu et al. (2010) explored the effect of ALA (10 mg/kg/day) and vitamin C (25 mg/kg/day) on arsenic (50 mg/L water) induced oxidative stress. It was observed that the combination of both the antioxidants significantly decreased the TBARS level of the brain and liver and thereby attenuated oxidative stress, restored the δ-ALAD activity against arsenite induced toxicity (Liu et al., 2010). Investigation of influence of ALA treatment in malathion (100 mg/kg) induced toxicity revealed that the pretreatment with ALA significantly attenuated the physiological and histopathological alterations induced by malathion (Al-Attar, 2010). ALA was reported to exhibit protective effect against combination of Isoniazid and Rifampicin (INH-RIF) induced hepatotoxicity (Saad et al., 2010).

In the present study, supplementation with ALA (200 mg/kg) decreased the markers of hepatotoxicity such as SGOT, SGPT and bilirubin which were elevated by phenytoin. ALA supplementation also restored the levels of albumin and total protein decreased by phenytoin. In addition, ALA restored the total body weight of the rats and decreased the relative liver weight against phenytoin induced alterations. ALA also has improved the hepatic histopathological damages induced by phenytoin. ALA at the dose of 200 mg/kg exerted significant protection against phenytoin induced toxicity by its ability to ameliorate the lipid peroxidation and thus oxidative stress through its free radical scavenging activity, which improved the levels of antioxidant defense system.

Conclusion

The results of the present investigation revealed the protective effect of ALA against phenytoin induced oxidative stress and hepatotoxicity. ALA also reversed the histopathological damages induced by phenytoin in liver. ALA at a dose of 100 and 200 mg/kg was effective in reducing the oxidative stress and hepatic damage. The enzyme inducing property of phenytoin might possibly explain the relative inefficiency of ALA at 50 mg/kg. This investigation reports the beneficial ALA on phenytoin induced hepatotoxicity mediated via oxidative stress.

REFERENCES

Al-Attar AM (2010). Physiological and histopathological investigations on the effects of ALA in rats exposed to malathion. J. Biomed. Biotechnol. 1-8.

Aldenhovel HG (1988). The influence of long-term anticonvulsant therapy with diphenylhydantoin and carbamazepine on serum gamma glutamyl transferase, aspartate aminotransferase, alanine aminotransferase and ALP. Eur. Arch. Psychiatry Neurol. Sci. 237(5):312-316.

Bajpai M, Roskos LK, Shen DD, Levy RH (1996). Roles of cytochrome P_{450}2C9 and cytochrome P_{450}2C19 in the stereoselective metabolism of Phenytoin to its major metabolite. Drug Metab. Dispos. 24(12):1401-1403.

Bavdekar SB, Muranjan MN, Gogtay NJ, Kantharia V, Kshirsagar NA (2004). Anticonvulsant hypersensitivity syndrome: lymphocyte toxicity assay for the confirmation of diagnosis and risk assessment. Ann. Pharmacother. 38(10):1648-1650.

Beer RF, Sizer IW (1952). A spectrophotometric method for measuring the breakdown hydrogen peroxide by catalase. J. Biol. Chem. 195(1):133-140.

Björnsson E (2008). Hepatotoxicity associated with antiepileptic drugs. Acta Neurol. Scand. 118(5):281-290.

Chatterjee M, Sil PC (2006). Hepatoprotective effect of aqueous extract of Phyllanthus niruri on nimesulide induced oxidative stress in vivo. Indian J. Biochem. Biophys. 43(5):299-305.

Doumasa BT, Watson WA, Biggs HG (1971). Albumin standards and the measurement of serum albumin with bromocresol green. Clin. Chim. Acta 31(1):87-96.

Dreifuss FE, Langer DH (1987). Hepatic considerations in the use of antiepileptic drugs. Epilepsia 28(2):S23-S29.

Eraslan G, Kanbur M, Silici S (2009). Effect of carbaryl on some biochemical changes in rats: the ameliorative effect of bee pollen. Food Chem. Toxicol. 47(1):86-91.

Foo NP, Lin SH, Lee YH, Wu MJ, Wang YJ (2011). α-Lipoic acid inhibits liver fibrosis through the attenuation of ROS-triggered signaling in hepatic stellate cells activated by PDGF and TGF-β. Toxicology 282(1-2):39-46.

Gella FJ, Olivella T, Cruz Pastor M, Arenas J, Moreno R, Dueban R, Gomez JA (1985). A simple procedure for routine determination of aspartate aminotrasferase and alanine aminotransferase with pyridoxal phosphate. Clin. Chim. Acta 153(3):241-247.

George J, Farrell GC (1994). Anticonvulsivant hepatotoxicity. In: Farrell GC (ed.), Drug-induced Liver Disease. Churchill Livingstone, Edinburgh, London. pp. 143-144.

Gokcimen A, Gulle K, Demirin H, Bayram D, Kocak A, Altuntas I (2007). Effects of diazinon at different doses on rat liver and pancreas tissues. Pestic. Biochem. Physiol. 87(2):103-108.

Gomall AG, Bardawill CJ, David MM (1949). Determination of serum proteins by means of biuret reaction. J. Biol. Chem. 177(2):751-766.

Harden CL (2000). Therapeutic safety monitoring: what to look for and when to look for it. Epilepsia 41(8):S37-S44.

Hesham AEB (2007). Lipoic acid attenuates DNA fragmentation, oxidative stress and liver injury induced by tamoxifen in rats. Asian J. Tradit. Med. 2:175-188.

Kalapos MP (2002). Carbamazepine provoked hepatotoxicity and possible etiopathological role of glutathione in the events. Retrospective review of old data and call for new investigation. Adv. Drug React. Toxicol. Rev. 21(3):123-141.

Kass GE (2006). Mitochondrial involvement in drug-induced hepatic injury. Chem. Biol. Interact. 163(1), 145-159.

Kazamatsuri H (1970). Elevated serum ALP levels in epilepsy during diphenylhydantoin therapy. N. Engl. J. Med. 283(25):1411-1412.

Li Y, Powers C, Jiang N, Chopp M (1998). Intact, injured, necrotic and apoptotic cells after focal cerebral ischemia in the rat. J. Neurol. Sci. 156(2):119-132.

Liu CB, Feng YH, Ye GH, Xiao M (2010). Effects of α-lipoic acid and vitamin C on oxidative stress in rat exposed to chronic arsenic toxicity. Zhonghua Lao Dong Wei Sheng Zhi Ye Bing Za Zhi 28(12):891-894.

Lowry OH, Rosebrough NJ, Farr AL, Randall RJ (1951). Protein measurement with the Folin phenol reagent. J. Biol. Chem. 193(1):265-75.

Madden S, Maggs JL, Park BK, (1996). Bioactivation of carbamazepine in the rat invivo. Evidence for the formation of reactive arene oxide(s). Drug Metab. Dispos. 24(4):469-479.

Marklund S, Marklund G (1974). Involvement of the superoxide anion radical in the auto oxidation of pyragallol and a convenient assay for superoxide dismutase. Eur. J. Biochem. 47(3):469-474.

Ncibi S, Othman MB, Akacha A, Krifi MN, Zourgui L (2008). Opuntia ficus indica extract protects against chlorpyrifos-induced damage on mice liver. Food Chem. Toxicol. 46(2):797-802.

Packer L, Witt EH, Tritschler HJ (1995). Alpha-lipoic acid as a biological antioxidant. Free Radic. Biol. Med. 19(2):227-250.

Pari L, Murugavel P (2004). Protective effect of alpha lipoic acid against chloroquine induced hepatotoxicity in rats. J. Appl. Toxicol. 24(1):21-26.

Pearlman FC, Lee RTY (1974). Detection and measurement of total bilirubin in serum with use of surfactants as solubilizing agents. Clin. Chem. 20(4):447-453.

Rosalki SB, Foo AY, Burlina A, Prellwitz W, Strieber P, Neumeier D, Klein G, Poppe WA, Bodenmuller H (1993). Multicentre evaluation of iso ALP test kit for measurement of bone alkaline phosphatase ativity in serum and plasma. Clin. Chem. 39(4):648-652.

Roy D, Snodgrass WR (1988). Phenytoin metabolic activation: role of cytochrome P450, glutathione, age, and sex in rats and mice. Res. Commun. Chem. Pathol. Pharmacol. 59:173-190.

Saad EI, El-Gowilly SM, Sherhaa MO, Bistawroos AE (2010). Role of oxidative stress and nitric oxide in the protective effects of alpha-lipoic acid and aminoguanidine against isoniazid rifampicin induced hepatotoxicity in rats. Food Chem. Toxicol. 48(7):1869-1875.

Sallie R, Tredger JM, Willam R (1991). Drugs and the Liver. Biopharm. Drug Dispos. 12:251-259.

Santos NA, Medina WS, Martins NM, Rodrigues MA, Curti C, Santos AC (2008). Involvement of oxidative stress in the hepatotoxicity induced by aromatic antiepileptic drugs. Toxicol. Vitro 22(8):1820-1824.

Saraswathy GR, Maheswari E, Santhrani T (2010). Effect of Vitamin C supplementation on phenytoin induced hepatotoxicity. Glob. J. Pharmacol. 4(3):127-135.

Sedlak J, Lindsay RH (1968). Estimation of total, protein bound & non-protein SH groups in tissue with Ellman's reagent. Anal. Biochem. 25(1):192-205.

Shear NH, Spielberg SP (1988). Anticonvulsant hypersensitivity syndrome. *In vitro* assessment of risk. J. Clin. Investig. 82(6):1826-1832.

Smythe MA, Umstead GS (1989). Phenytoin hepatotoxicity: a review of the literature. DICP 23(1):13-18.

Kalender S, Gokce Uzun F, Durak D, Demir F, Kalender Y (2010). Malathion-induced hepatotoxicity in rats: The effects of vitamins C and E. Food Chem. Toxicol. 48(2):633-638.

Walia KS, Khan EA, Ko DH, Raza SS, Khan YN (2004). Side effects of antiepileptics - a review. Pain Pract. 4(3):194-203.

Walker M (2005). Status epilepticus: an evidence based guide. BMJ 331(7518):673–677.

Zaccara G, Franciotta D, Perucca E (2007). Idiosyncratic adverse reactions to antiepileptic drugs. Epilepsia 48(7):1223-1244.

academicJournals

Vol. 9(7), pp. 205-208, 22 February, 2015
DOI: 10.5897/AJPP2014. 4281
Article Number: 36B79FA51239
ISSN 1996-0816

http://www.academicjournals.org/AJPP

African Journal of Pharmacy and Pharmacology

Full Length Research Paper

Phytochemical screening and analgesic properties of ethanol extract of the leaves of *Hugonia mystax* L.

M. Mohankumar

Department of Pharmaceutical Chemistry, Nandha College of Pharmacy, Erode-52, India.

Received 25 January, 2015; Accepted 3 February, 2015

***Hugonia mystax (H. mystax)* has been used in the siddha and ayurvedha for various ailments. In this study ethanolic crude extract (EEHM) of the leaves were studied for various analgesic methods. The ethanolic extract of *H. mystax* was spiked into the male swiss albino mice (weighing 20 to 25 g) and male wister rats weighing (150 to 200 g) and analyzed the analgesic activity by hot plate and acetic acid induced method. The phytochemical analysis of ethanolic extract of *H. mystax* showed the presence of carbohydrates, flavonoids, steroids, saponins, terpenoids and absence of alkaloids, proteins and amino acids. For acute toxicity test, mice were injected different doses of each extract by intraperitoneal route and the LD_{50} values were determined. The analgesic effect was evaluated in mice by the hot plate method and acetic-acid writhing test. The extracts have produced significant analgesic effects by the acetic acid writhing test and by the hot plate method (p <0.01) and a dose-dependent inhibition was observed. The overall results indicate the significant analgesic activity and also its justification for further traditional uses *H. mystax* leaves.**

Key words: *Hugonia mystax*, analgesic activity, toxicity.

INTRODUCTION

The genus *Hugonia* L. of family Linaceae comprise about 40 species in the world; of which *Hugonia mystax* L. was reported from India and Srilanka (Santapau and Henry, 1983; Pullaiah and Chennaiah, 1997). This plant *H. mystax* is locally named Modirakanni. Ethno botanically, the fruits were used by the tribals of Kalakad Mundanthurai for the treatment of rheumatism (Sutha et al., 2009). The literature study reveals that the roots of *H. mystax* were used as anthelmintic, astringent and also used for dysentery, snake bite, fever, inflammation and rheumatism. Biological activities such as analgesic, anti inflammatory and ulcerogenic were also reported (Balasubramaniam et al., 1997; Guha et al., 2001). The anti-oxidant activity was confirmed by the studies on the leaf (Rajeswari et al., 2013). Antimicrobial activity of petroleum ether, chloroform, ethanol and aqueous extracts of root extracts showed significant activity against various human pathogens (Vimalavady et al., 2012). Preliminary phytochemical screening showed the presence of various classes of secondary metabolites such as flavonoids, phenols, saponins, steroids, tannins and terpenoids. The bioactive components are identified through by the gas chromatography-mass spectrometry (GC-MS) analysis (Kaneria et al., 2007).

E-mail: mmkpy6@gmail.com. Tel: 99433-36384.

The drug compendium (Rastogi et al., 2002; Yoganarasimhan, 2000) showed the leaves of *H. mystax* has an analgesic activity but there is no study reported. With addition to the fact that the compound containing analgesic activity nature was phytochemically identified in the ethanol extracts of leaf of *H. mystax* (Rajeswari et al., 2012) by GC-MS analysis and the result showed the *H. mystax* leaves containing the isoprenoid compound. Many of the studies showed that the chemical nature of isoprenoid have the analgesic character (Damiao, 2011; Magdalena et al., 2013; UIC, 2014). The compounds of squalene and vitamin E (Rajeswari et al., 2012; Damiao, 2011; Magdalena et al., 2013; UIC, 2014) have the isoprenoid units which was present in the leaves of *H. mystax*. So we can make attempt by this analgesic character, later on the leaves extract showed the good result in the trail works. So, we take this as the consideration and also on the medicinal value and utility. The present study was aimed to explore the analgesic activity of the medicinal plant named *H. mystax*. The objective of the work was to prove the analgesic activity of *H. mystax* leaves through the techniques of hot plate and acetic acid induced method.

MATERIALS AND METHODS

Collection, identification and preparation of plant materials

Fresh leaves of *H. mystax* were collected from velliangiri hills from Coimbatore, Tamilnadu. It was identified by a scientific officer, Dr. P.Samydurai Assistant Professor, Department of Botany, Kongu Nadu Arts and Science College, Coimbatore. The identification was confirmed with Botanical Survey of India (BSI), Coimbatore, TamilNadu, India. The reference number was: BSI/SRC/5/23/10-11/Tech-1522. The herbarium specimen of *H. mystax* was prepared and deposited in the department of Pharmacology, Nandha College of Pharmacy and Research Institute, Erode, India for future reference.

Animals

Male swiss albino mice weighing 20 to 25 g and male wister rats weighing 150 to 200 g was used for this study. The animals were obtained from animal house, Nandha College of Pharmacy, Erode, Tamilnadu. The experimental procedures and protocols used in this present study were reviewed by institutional animal ethical committee (688/2/C-CPCSEA) of Nandha College of Pharmacy and the proposal number was (NCP/IAEC/PG-40/2009) and also in accordance with the guidelines of Institute for Animal Care Education (IACE). Animals were housed at a temperature of 24 ± 2°C and relative humidity of 30 to 70%. A 12:12 light: day cycle was followed. All the animals were allowed free access to water and fed with standard commercial pelleted chaw (M/s. Hindustan Lever Ltd., Mumbai). The present work was conducted with an effort to minimize the usage of number of animals and the suffering caused by the used procedures in the study.

Preparation of extracts

Leaves of *H. mystax* were dried in shade for two weeks. Dried leaves were coarsely powdered, sieved (#40) and stored in an air tight container at room temperature. Dried powder was then extracted sequentially with petroleum ether, chloroform and ethanol using soxhlation method. The extracts were concentrated to dryness using rotary evaporator. The yields of various extracts were found to be 4.5% w/w (petroleum ether), 4.7% w/w (chloroform) and 10.5% w/w (ethanol). All the extracts were preserved in a refrigerator at 4°C. However, only ethanolic extract of the leaves was selected for further studies.

Qualitative phytochemical analysis

The leaves of *H. mystax* was extracted by the continuous hot percolation method. The ethanolic extract of *H. mystax* was subjected to preliminary phytochemical screening to identify the different phytoconstituents like flavonoids, phenols, saponins, steroids, tannins and terpenoids.

Acute toxicity study

Acute toxicity study was carried out as per stair case method (as per Organisation for Economic Co-operation and Development (OECD) guidelines 425). Albino mice of either sex 20 to 25 g were used. The animals were fasted overnight prior to the acute experimental procedure. The animals were administered with aliquot doses of 100 to 250 mg/kg extracts orally, suspended in Tween 80 (1% w/v). The dose which caused no mortality and was tolerated was determined in a stepwise manner and the effective dose was found to be 100 mg/kg b.w. so that 100 and 200 mg/kg b.w. was selected for further studies.

Analgesic activity

Hot plate method

The paws of mice and rats are very sensitive to heat at temperatures which are not damaging to the skin. The responses are jumping, withdrawal of the paws and licking of the paws. The hot plate method was employed for the purpose of preferential assessment of possible centrally mediated analgesic effects of the ethanolic extract of *H. mystax*. The central analgesic drug pentazocine was used for positive control group. In this experiment, four groups (n = 6) of swiss albino mice (20 to 25 g) were placed on a hot plate maintained at room temperature for 15 min. The controlled temperature of commercially available Eddy's hot plate is 55 to 56°C (Rajeswari et al., 2014).

Grouping of animals

Group 1 – Received normal control (0.5% CMC p.o.)
Group 2 – Received Pentazocin (30 mg/kg i.p.)
Group 3 – Received Ethanolic extract of *H. mystax* (100 mg/kg, p.o.)
Group 4 - Received Ethanolic extract of *H. mystax* (200 mg/kg, p.o.)

The observations were recorded and the time interval of 15, 30, 45 and 60 min, respectively. The results of hot plate method in swiss albino mice were tabulated in Table 1.

Acetic acid induced writhing in mice

Pain is induced by injection of irritants into the peritoneal cavity of mice. The animals react with a characteristic stretching behavior which is called writhing. The test is suitable to detect analgesic

Table 1. Analgesic activity of ethanolic extract of *H. mystax* by hot plate method.

Treatment	Reaction time (min)			
	15	**30**	**45**	**60**
Control (0.5% CMC)	2.2 ± 0.2	2.4 ± 0.1	2.5 ± 0.2	2.4 ± 0.4
Pentazocine (30 mg/kg)	4.4 ± 0.4[b]	5.4 ± 0.2[b]	6.2 ± 0.4[b]	8.2 ± 0.6[b]
EEHM (100 mg/kg)	4.2 ± 0.3[b]	5.0 ± 0.2[b]	5.8 ± 0.3[b]	7.4 ± 0.3[b]
EEHM (200 mg/kg)	4.3 ± 0.3[b]	5.3 ± 0.2[b]	6.0 ± 0.1[b]	8.0 ± 0.2[b]

The data represent the Mean ± SEM (n=6), $p<0.05^c$, $p<0.01^b$, $p<0.001^a$ when compared to control. (One way ANOVA followed by Tukey T test).

Table 2. Analgesic activity of ethanolic extract of *H. mystax* by acetic acid induced writhing method.

Treatment	Number of writhing	% Inhibition
Control (0.5% CMC)	65.67 ± 0.5	-
Indomethacine (5mg/kg)	19.57 ± 0.5[b]	72
EEHM (100 mg/kg)	35.32 ± 0.5[b]	47
EEHM (200 mg/kg)	23.65 ± 0.7[b]	65

The data represent the mean ± SEM (n = 6), $p < 0.05^c$, $p < 0.01^b$, $p < 0.001^a$ when compared to control.

activity. An irritating agent such as acetic acid is injected intra-peritoneally to mice and stretching reaction is evaluated (Shanmugasundaram and Venkataraman, 2005).

Grouping of animals

Group 1 – Received normal control (0.5% CMC p.o.).
Group 2 – Received Indomethacin (5 mg/kg p.o.).
Group 3 – Received Ethanolic extract of *H. mystax* (100 mg/kg, p.o.).
Group 4 - Received Ethanolic extract of *H. mystax* (200 mg/kg, p.o.).

Swiss albino mice of male sex were divided into four different groups each containing six animals. Food was withdrawn 12 h prior to drug administration till completion of experiment. The animals were weighed and numbered appropriately. The test and standard drugs were given orally. The central analgesic drug indomethacine was used for positive control group. After 60 min, writhing was induced by intraperitonial injection of 1% acetic acid in volume of 0.1 ml/10 g body weight. The writhing episodes were recorded for 30 min; stretching movements consisting of arching of the back, elongation of body and extension of hind limbs were counted. The result of acetic acid induced writhing method in mice was tabulated in Table 2.

RESULTS AND DISCUSSION

The analgesic activity of ethanolic extract of *H. mystax* by hot plate method test indicated a significant increase in reaction time ($p < 0.01$) at the dose of 100 and 200 mg/kg comparable to control. In acute toxicity study, no toxic symptoms were observed for the drug up to 2000 mg/kg body weight. The activity produced by the standard pentazocine was found to be the highest reaction time among the group tested. Prostaglandins and bradykinins were suggested to play an important role in pain. The hot plate test was selected to investigate central anti-nociceptive activity because it had several advantages particularly the sensitivity to strong antinociceptive and limited tissue damage. The ethanolic extract of *H. mystax* showed significant analgesic activity by acetic acid induced writhing method. The oral administration of ethanolic extract of *H. mystax* induced a dose dependent analgesic activity. Injection of acetic acid into control mice produced 65.67 ± 0.5 writhes. Pretreatment with ethanolic extract of *H. mystax* at doses of 100 and 200 mg/kg reduced the number of writhes by 35.32 ± 0.5 (47% protection) and 23.65 ± 0.7 (65%), respectively.

Conclusion

From the investigation, the ethanolic extract of *H. mystax* leaves possesses potent analgesic effect against differrent stimuli. This is evidenced by significant increase in the reaction time by stimuli in different experimental models.

ACKNOWLEDGEMENTS

The authors are well acknowledged to the management of Nandha College of Pharmacy and Research Institute, Erode, Tamil Nadu, India and NRK and KSR Gupta College of Pharmacy, Tenali, Andhra Pradesh, India for providing necessary laboratory facilities in the department and their support.

Conflict of interest

There is no conflict of interest as regard this study.

REFERENCES

Balasubramaniam P, Rajasekaran A, Prasad SN (1997). Folk Medicine of the Irulas of Coimbatore Forests. Anc. Sci. Life 16(3):222-226.

Damiao PDS (2011). Analgesic-like Activity of Essential Oils Constituents. Molecules, 16**:**2233-2252.

Guha BDN, Sensarma P, Pal DC (2001). Lexicon of Medicinal Plants in India. Calcutta, India, Naya Prokash Publishers. Vol. 2, P 369.

Kaneria MS, Naik SR, Kohli RK (2007). Anti-inflammatory, antiarthritic and analgesic activity of a herbal formulation. Ind. J. Exp. Biol. 45(3):278-284.

Magdalena M, Elżbieta S, Jan O (2013). Production of triterpenoids with cell and tissue cultures. Acta Biochim. Pol. 60(4):731–735.

University of Illinois, UIC (2014). Vitamin E - Structures and Chemistry. Available at: https://www.uic.edu/classes/phar/phar332/Clinical_Cases/vitamin%20cases/vitamin%20E/Vitamin%20E%20Chemistry.htm. Accessed June 2014.

Pullaiah T, Chennaiah E (1997). Flora of Andhra Pradesh. Scientific Publishers, Jodhpur, India.

Rajeswari G, Murugan M, Mohan VR (2012). GC-MS analysis of bioactive components of *Hugonia mystax L*. (Linaceae). Res. J. Pharm. Biol. Chem. Sci. 3(4):301-308.

Rajeswari G, Murugan M, Mohan VR (2013). GC-MS analysis of bioactive components of Hugonia mystax L. bark (Linaceae). J. Pharm. Biomed. Sci. 29(29):818-824.

Rajeswari G, Murugan M, Mohan VR (2014). Total phenolic and flavonoid contents and in vitro antioxidant activity of *Hugonia mystax* linn leaf (linaceae). Int. J. Preclil Pharm. Res. 5(1):12-18.

Rastogi P, Mehrotra BN, Sinha S, Srivastava M, Bhushan B (2002). Compendium of Indian Medicinal Plants. Lucknow, *CDRI*, 4:386.

Santapau H, Henry AN (1983). A Dictionary of flowering plants in India. Council of Scientific and Industrial Research (CSIR), New Delhi. P 103.

Shanmugasundaram P, Venkataraman S (2005). Anti-nociceptive activity of Hygrophila auriculata (SCHUM) Heine. Afr. J. Tradit. Complement. Altern. Med. 2(1):62-69.

Sutha S, Mohan VR, Kumaresan S, Murugan C, Athiperumalsami T (2009). Ethnomedicinal plants used by the tribals of Kalakad Mundanthurai Tiger Reserve (KMTR), Western Ghats, Tamil Nadu for the treatment of rheumatism. Ind. J. Tradit. Knowl. 9(3):502-509.

Vimalavady A, Kadavul K, Tangavelou AC (2012). Phytochemical screening and antimicrobial activity on the fruits of *Hugonia mystax* L. (Linaceae). Int. J. Pharm. Sci. Res. 3(2):1178-1183.

Yoganarasimhan SN (2000). Medicinal Plants of India. Bangalore, India. Vol. 2, P 275.

academicJournals

Vol. 9(7), pp. 209-222, 22 February, 2015
DOI: 10.5897/AJPP2014. 4261
Article Number: xxxxx
ISSN 1996-0816

http://www.academicjournals.org/AJPP

African Journal of Pharmacy and Pharmacology

Full Length Research Paper

Synthesis, *in-vitro*, *in-vivo* evaluation and molecular docking of 2-(3-(2-(1, 3-dioxoisoindolin-2-yl) acetamido)-4-oxo-2-substituted thiazolidin-5-yl) acetic acid derivatives as anti-inflammatory agents

Anna Pratima Nikalje[1]*, Nazma Hirani[2] and R. Nawle[3]

[1]Department of Pharmaceutical Chemistry, Y.B. Chavan College of Pharmacy, Dr. Rafiq Zakaria Campus, Rauza Bagh, P.B. No. 33, Aurangabad-431001, Maharashtra, India.
[2]Department of Pharmacology, Y.B. Chavan College of Pharmacy, Dr. Rafiq Zakaria Campus, Rauza Bagh, P.B. No. 33, Aurangabad-431001, Maharashtra, India.
[3]Department of Pharmacology, Government College of Pharmacy, Aurangabad-431001, Maharashtra, India.

Received 30 December, 2014; Accepted 21 January, 2015

A series of novel 2-(3-(2-(1,3-dioxoisoindolin-2-yl) acetamido)-4-oxo-2-phenylthiazolidin-5-yl) acetic acid (5a-l) have been synthesized by cyclocondensation of *N*-substituted benzylidene/methylene-2-(1,3-dioxo isoindolin-2-yl) acetohydrazide (4a-l) with mercapto succinic acid in dimethylformamide (DMF) as solvent and using anhydrous zinc chloride as a catalyst in microsynth microwave reactor. The synthesized compounds were evaluated for anti-inflammatory activity using *in vitro* and *in vivo* model. Furthermore, ulcerogenic toxicity study was performed for selected compounds. All the compounds have shown promising anti-inflammatory activity in both the models. Docking studies were performed to know the binding affinity towards the human serum albumin (HSA).

Key words: Thiazolidinone, microwave assisted, anti-inflammatory, protein denaturation, rat paw edema, molecular docking.

INTRODUCTION

Non steroidal anti-inflammatory drugs (NSAIDs) are one of the most commonly used therapeutically important agents for the treatment of pain, fever and inflammation (Madhukar et al., 2010). The usefulness of these agents is limited due to the side effects like gastric ulceration (Lombardino, 1985), gastro intestinal (GI) bleeding (Pilotto et al., 1997) and suppression of renal function (Pirson et al., 1986), and these side effects are related to their intrinsic mechanism of action.

From the literature survey, it was observed that both phthalimide and thiazolidinone derivatives are potentially useful as anti-inflammatory agents (Pawar and Chavan, 2012; Bhalgat et al., 2011; Bosquesi et al., 2011; Pophale and Deodhar, 2010; Machado et al., 2005; Alanazi et al., 2015; Vigorita et al., 2002; Ottana et al., 2005; Bhat and Kumar, 2008; Amin et al., 2010; Unsal et al., 2012; Hu et

*Corresponding author. E-mail: annapratimanikalje@gmail.com. Tel: +91 9823619992.

al., 2013; Singh et al., 2014; Thomas et al., 2013; Ahmed et al., 2013). Thiazolidinone scaffold is very versatile and is present in a number of clinically used drugs. They have varied applications as antimicrobial activity (Balzarini et al., 2007), anti-HIV activity (Monforte, 2001), antimalarial activity (Solomon et al., 2013), anti cancer activity (Gududuru et al., 2004) and antiarrhythmic activity (Jackson et al., 2007). Furthermore, it was observed that aryl acetic acid and α-methyl aryl acetic acid derivatives have high degree of potency as anti- inflammatory agents. In the present work, our objective was to design and synthesize a series of novel acetic acid derivatives containing thiazolidinone ring and couple this moiety with phthalimide ring (dioxoisoindoline) through the amide linkage so as to get the coupled derivatives with enhanced bioactivity. The compounds were designed such that -CH_2COOH group is at C5 position of thiazolidinone ring, various alkyl/aryl/heteryl groups at C2 position of thiazolidinone ring.

We report here the synthesis, docking studies, anti inflammatory activity and ulcerogenic toxicity of these novel thiazolidinone-5-yl acetic acid analogues. The anti-inflammatory activity was assessed, *in silico*, to know the binding and affinity towards the human serum albumin (HSA), *in vivo* by using carrageenan induced rat paw edema model, *in vitro* through protein denaturation inhibition assay using albumin.

EXPERIMENTALS

All chemicals were purchased from commercial suppliers and used without further purification. Nuclear magnetic resonance (NMR) spectra were recorded on a VARIAN MERCURY YH 300 Spectrometer at 300MHz. Chemical shifts are reported in parts per million (ppm), using TMS as an internal standard and $CDCl_3$ as a solvent. ^{13}C spectra were recorded on AVANCE spectrometer at 300 MHz using $CDCl_3$ as a solvent. Infrared (IR) spectra were recorded for the compounds on JASCO Fourier transform infrared spectroscopy (FTIR) (PS 4000) using KBr pallet, mass spectra were recorded on GC-AccuTOF GC- high resolution, EI system. The homogeneity of the compounds was monitored by ascending thin layer chromatography (TLC) on silica gel-G (Merck) coated aluminum plates, visualized by iodine vapor. Elemental analyses (C, H, and N) were undertaken with a Shimadzu's FLASHEA112 analyzer and all analyses were consistent with theoretical values (within ± 0.4%) unless indicated. Digital plethysmometer (Ugo Basil 7140, Italy) was used for evaluation of anti-inflammatory activity.

General procedure for the preparation of N-substituted benzylidene/methylene-2-(1, 3-dioxo isoindolin-2-yl) acetohydrazides (4a-l)

2-(1, 3-Dioxoisoindolin-2-yl) acetic acid 1 was obtained by the reaction of phthalic anhydride (0.05 mol) with glycine (0.05 mol) (Furniss et al., 1998). Ethyl 2-(1,3-dioxoisoindolin-2-yl) acetate 2 was synthesized by refluxing 2-(1,3-Dioxoisoindolin-2-yl) acetic acid with conc. H_2SO_4 in ethanol for 2hrs by conventional route (Amir and Shikha, 2004) in preparation of 2-(1,3-dioxoisoindolin-2-yl) acetohydrazide 3. The drawback of conventional method was lump formation upon refluxing and time required was 6 to 8 h. Therefore, to avoid lump formation, reaction was carried out at room temperature with continuous stirring and adding hydrazine hydrate to the compound 2 in ethanol. The Schiff bases were obtained by condensing aldehyde (0.03 mol) with compound 3 in ethanol for 6 to 8 h, in presence of glacial acetic acid (0.06 mol) as catalyst. Products were recrystallized with ethanol. The other compounds 4(a-l) were prepared similarly by treating with various substituted aliphatic, aromatic and heterocyclic aldehydes.

General procedure for the preparation of 2-(3-(2-(1,3-dioxoisoindolin-2-yl) acetamido)-4-oxo-2-substituted thiazolidin-5-yl) acetic acid 5(a-l)

Phthalic anhydride (2.96 g, 0.02 mol) and glycine (1.5 g, 0.02 mol) were suspended in glacial acetic acid (20 ml). The suspension was refluxed for 8 h on water bath and then cooled to room temperature. The completion of reaction was monitored by thin layer chromatography (TLC). The cooled mixture was poured into ice water (20 ml). The resulting product (1) was filtered, washed with water and dried. The solid was recrystallized from hot water. The melting point and yield were recorded. Alternatively, when mixture of phthalic anhydride (2.96 g, 0.02 mol) and glycine (1.5 g, 0.02 mol) was irradiated in Erlenmeyer flask in microwave oven for 30 min at high power, 700 W, after cooling the reaction mixture was poured in cold water to obtain 2-(1,3-Dioxoisoindoline-2-yl)acetic acid compound (1). The solid was recrystallized from hot water. The melting point and yield were recorded. Melting point (MP) is 194 to 196°C. Yield: Conventional - 89%; Microwave - 98%.

Compound (1) and Conc. H_2SO_4, both 0.01 mol, were refluxed in ethanol for 2 h. The reaction was monitored by TLC. The cooled mixture was poured into 100 ml ice water. The solid obtained was filtered, washed with saturated sodium bicarbonate solution, followed by washing with water and dried to get compound ethyl -(1,3-dioxoisoindoline-2-yl)acetate (2). It was recrystallized from ethanol and MP was recorded 121°C, yield 89%. This compound (0.01 mol) was stirred in absolute ethanol and hydrazine hydrate (0.02 mol) was added drop wise with constant stirring for 1 h at room temperature. The solid appeared is 2-(1,3-dioxoisoindolin-2-yl) acetohydrazide (3) was filtered, dried and recrystallized from rectified spirit and melting point was recorded as 176°C, yield 87%.

Equimolar quantities of (3) and various aliphatic/and aromatic aldehyde (0.01 mol) were refluxed in absolute ethanol (25 ml) for 6 to 8 h, in presence of few drops of glacial acetic acid as a catalyst. The completion of reaction was monitored by TLC. The reaction mixture was concentrated and poured into ice cold water. The obtained solid was filtered and washed with saturated solution of sodium meta bisulphate to remove any traces of un reacted aldehyde, then washed with water and dried and the compound (4) thus obtained was recrystallized by ethanol. Similarly, other derivatives of *N*-substituted benzylidene/methylene-2-(1,3-dioxoisoindolin-2-yl) acetohydrazide 4(a-l) were prepared. The data for yield and melting point for these compounds were as follows: 4a- 72%, 226°C, 4b- 76%, 232°C, 4c- 89% 218°C, 4d- 80%, 210°C, 4e- 72%, 237°C, 4f- 85%, 296°C, 4g- 87%, 224°C, 4h- 87%, 200°C, 4i- 83%, 254°C, 4j- 85%, 240°C, 4k- 79%, 192°C , 4l- 85%, 274°C.

The final derivatives, 2-(3-(2-(1,3-dioxoisoindolin- 2-yl) acetamido)-4-oxo-2-substituted thiazolidin-5-yl) acetic acid 5(a-l) were obtained under microwave irradiation by cyclo-condensation of *N*-substituted benzylidene/methylene-2-(1,3-dioxoisoindolin-2-yl) acetohydrazide (4) taken 0.01 mol with mercapto succinic acid (0.015 mol) in 20 ml DMF as solvent and anhydrous zinc chloride, as catalyst in Microsynth microwave reactor for about 14 to 17 min (700 W) at 80°C. After completion of reaction (monitored by TLC), the mixture was poured into ice cold water. The solid product formed was filtered, dried and recrystallized by ethanol. The yield and melting point were recorded.

2-(3-(2-(1, 3-Dioxoisoindolin-2-yl)acetamido)-2-methyl-4-oxothiazolidin-5-yl)acetic acid (5a)

IR (KBr): *v*/cm^{-1}, 3500 (OH of carboxyl), 3251 (NH of amide), 3021 (C-H of aromatic), 2975 (C-H of alkyl), 1768 (C=O of thiazolidinone), 1725-1728 (C=O of Phthalimide),1716(C=O of carboxyl), 1664(C=O of Amide),746 (C-S).1H NMR (CDCl3, 300 MHz) δ ppm: 10 (s, 1H, OH), 8.0-8.2(s, 1H, NH), 7.2-7.4 (m, 4H Ar-H), 5.0(s, 2H, -CH_2), 4.3-4.6(quar, 1H, -CH), 3.4-3.6(t, 1H,-CH), 2.6-2.8(d, 2H, -CH_2), 1.5 (s, 3H, CH_3). ^{13}CNMR (CDCl3, 300 MHz) δ ppm: 175.3 (carboxyl group), 173.0 (carbonyl of thiazolidinone ring), 170.3 (carbonyl of amide), 168.2 (two peaks carbonyl carbons of phthalimide ring),132.2, 132.0, 123.7 (aromatic ring carbon), 50.2 (-CH of thiazolidinone ring) 50.1 (-CH_2 near amide group) 39.2 (-CH_2 attached to carboxyl), 25.2 (-CH_3 of thiazolidinone ring).MS m/z %: M+ 377 100%, M+1 378 19.6%, 362 M-CH_3, 303, 203, 161(base peak). Anal. Calcd. for $C_{16}H_{15}N_3O_6$ S: C, 50.92; H, 4.01; N, 11.13, Found: C, 50.96 H, 4.04 N, 11.17.

2-(3-(2-(1,3-Dioxoisoindolin-2-yl)acetamido)-2-ethyl-4-oxothiazolidin-5-yl)acetic acid (5b)

IR (KBr): *v*/cm^{-1}, 3498 (OH of carboxyl), 3341(NH of amide), 3021 (C-H of aromatic),2901(C-H of alkyl) 1788(C=O of thiazolidinone), 1728(C=O of carboxyl)1724,1720 (C=O of Phthalimide), 1656 (C=O of Amide),749(C-S).1H NMR (CDCl3, 300 MHz) δ ppm: 10.1 (s, 1H, OH), 7.2-7.6(m, 4H, Ar-H), 7.68(s, 1H,-NH), 5.2(t, 1H,), 4.7(t, 1H, thiazolidinone ring), 4.3(s, 2H), 2.6-2.45 (d, 2H), 1.92(q, 2H, CH_2), 0.95(t, 3H, CH_3). ^{13}CNMR (CDCl3, 300 MHz) δ ppm: 175.3 (carboxyl group),173.0(carbonyl of thiazolidinone ring), 170.3(carbonyl of amide), 168.2(two peaks carbonyl carbons of phthalimide ring),132.2, 132.0, 123.7 (aromatic ring carbon), 61.0 , 47.6 (-CH of thiazolidinone ring) 50.1 (-CH_2 near amide group) 39.2 (-CH_2 attached to carboxyl), 28.6, 7.6 (-CH_2CH_3 of thiazolidinone ring).MS m/z: 391.08 100%, M+1:392.09 18.2%, 393.08 4.7%, 161. Anal. Calcd. for $C_{17}H_{17}N_3O_6$: S C, 52.17; H, 4.38; N, 10.74; Found: C, 52.13;H,4.34; N,10.71.

2-(3-(2-(1,3-Dioxoisoindolin-2-yl)acetamido)-4-oxo-2-phenylthiazolidin-5-yl)acetic acid (5c)

IR (KBr): *v*/cm^{-1}, 3528(OH of carboxyl), 3128 (NH of amide), 3011(C-H of aromatic) 2985(C-H of alkyl), 1760(C=O of thiazolidinone), 1733-1721 (C=O of Phthalimide), 1723(C=O of carboxyl), 1685(C=O of Amide), 737(C-S). 1H NMR (CDCl3, 300 MHz) δ ppm: 10.12 (s, 1H, OH), 8.17 (s, 1H -NH), 7.81 - 7.71 (m, 4H, Ar-H), 7.36-7.33 (m, 5H, Ar-H), 6.26 (d, 1H, -CH), 4.64 (s, 2H, -CH_2), 4.31 (t,1H, -CH), 2.27 (d, 1H, -CH). ^{13}CNMR (CDCl3, 300 MHz) δ ppm: 175.3 (carboxyl group),173.0(carbonyl of thiazolidinone ring), 170.3(carbonyl of amide), 168.2(two peaks carbonyl carbons of phthalimide ring), 138.2,132.2, 132.0,128.6,127.1,126.9, 123.7 (two aromatic rings carbon), 61.8 , 47.6 (-CH of thiazolidinone ring) 50.1 (-CH_2 near amide group) 39.2 (-CH_2 attached to carboxyl). MS m/z: 439.08 100%, 440.09 23.1%, 439,161. Anal. Calcd. for $C_{21}H_{17}N_3O_6$ S: C, 57.40; H, 3.90; N, 9.56; Found: C, 57.45; H, 3.93;N, 9.59.

2-(3-(2-(1,3-Dioxoisoindolin-2-yl)acetamido)-2-(4-hydroxyphenyl)-4-oxothiazolidin-5-yl)acetic acid (5d)

IR (KBr): *v*/cm^{-1}, 3540(OH of carboxyl), 3410(-OH group) 3281(NH of amide),, 3025(C-H of aromatic), 2912(C-H of alkyl), 1756 (C=O of thiazolidinone), 1724(C=O of carboxyl),1722,1715 (C=O of Phthalimide), 1666(C=O of Amide), 723(C-S).1H NMR (CDCl3, 300 MHz) δ ppm: 10.2(s, 1H, -OH carboxylic), 8.2(s, 1H, -NH), 7.2-7.4(m, 4H, Ar-H),6.7-7.7 (m, 4H, aromatic ring), 5.7(s, 1H, -OH phenolic), 5.0(s, 2H, -CH of thiazolidinone ring) , 4.9(s, 1H, -CH_2 near amide group), 3.8-4(t, 1H, -CH of thiazolidinone ring), 2.2-2.8(d, 2H,CH_2), ^{13}CNMR (CDCl3, 300 MHz) δ ppm: 175.3 (carboxyl group),173.0(carbonyl of thiazolidinone ring), 170.3(carbonyl of amide), 168.2(two peaks carbonyl carbons of phthalimide ring), 156.9,132.2, 132.0,131.8, 130.1, 115.8,127.1,126.9, 123.7 (two aromatic rings carbon), 61.8 , 47.6 (-CH of thiazolidinone ring) 50.1 (-CH_2 near amide group) 39.2 (-CH_2 attached to carboxyl). MS m/z: M+455.08 100% M+1456.08 25.1%, 439 M-OH, 363 M-PhOH, 304, 203, 161 (base peak). Anal. Calcd. for $C_{21}H_{17}N_3O_7$ S: C, 55.38; H, 3.76; N, 9.23; Found: C,55.41; H, 3.81;N 9.28.

2-(3-(2-(1,3-Dioxoisoindolin-2-yl)acetamido)-2-(3-hydroxyphenyl)-4-oxothiazolidin-5-yl)acetic acid (5e)

IR (KBr): *v*/cm^{-1}, 3457 (OH of carboxyl), 3346 (NH of amide), 3151 (C-H of aromatic), 2976 (C-H of alkyl), 1768 (C=O of thiazolidinone), 1730 (C=O of carboxyl) 1728, 1713 (C=O of Phthalimide), 1640 (C=O of amide), 716 (C-S). 1H NMR (CDCl3, 300 MHz) δ ppm: 10.2(s, 1H, -OH, carboxyl), 7.8-8.8 (m, 4H, Ar-H), 6.7-7.7 (m, 4H, aromatic ring), 7.33 (s, 1H, -NH), 6.52(s, 1H, -CH), 4.65(s, 2H, -CH_2) 4.31(t, 1H, -CH), 2.63(d, 2H,CH_2), ^{13}CNMR (CDCl3, 300 MHz) δ ppm: 175.3 (carboxyl group),173.0(carbonyl of thiazolidinone ring), 170.3(carbonyl of amide), 168.2(two peaks carbonyl carbons of phthalimide ring), 156.9,140.6, 132.2, 132.0,131.8, 130.1, 119.5, 123.7 114.4,114.3(two aromatic rings carbon), 62.1 , 47.6 (-CH of thiazolidinone ring) 50.1 (-CH_2 near amide group) 39.2 (-CH_2 attached to carboxyl). MS m/z: M+455.08 100% M+1456.08 25.1%, 439 M-OH, 363 M-PhOH, 304, 203, 161 (base peak). Anal. Calcd. for $C_{21}H_{17}N_3O_7$ S: C, 55.38; H, 3.76; N, 9.23; Found:C,55.34 H, 3.81;N,9.28.

2-(3-(2-(1, 3-Dioxoisoindolin-2-yl)acetamido)-2-(4-methoxyphenyl)-4-oxothiazolidin-5-yl)acetic acid (5f)

IR (KBr): *v*/cm^{-1}, 3596(OH of carboxyl), 3214(NH of amide), 3025(C-H of aromatic), 2894(C-H of alkyl) 1754(C=O of thiazolidinone), 1725(C=O of carboxyl), 1715,1713 (C=O of Phthalimide), 1663(C=O of amide), 742(C-S).1H NMR (CDCl3, 300 MHz) δ ppm: 10.23(s, 1H, -OH), 8.48.(s, 1H, -NH), 7.16-7.81 (m, 4H, Ar-H), 6.8-7.8(m, 4H, aromatic ring), 6.36(s, 1H, -CH, thiazolidinone ring), 4.65 (s, 2H, -CH_2 near amide group), 4.32(t, 1H, -CH, thiazolidinone ring), 3.8 (s, 3H, -OCH_3), 2.9-2.6(d, 2H,CH_2), ^{13}CNMR (CDCl3, 300 MHz) δ ppm: 175.3 (carboxyl group),173.0(carbonyl of thiazolidinone ring), 170.3(carbonyl of amide), 168.2(two peaks carbonyl carbons of phthalimide ring), 159.0, 132.2, 132.0,131.8, 131.5, 130.1, 129.7, 123.7 114.2, (two aromatic rings carbon), 61.8 , 47.6 (-CH of thiazolidinone ring), 55.8(-OCH_3), 50.1 (-CH_2 near amide group) 39.2 (-CH_2 attached to carboxyl). MS m/z: M+ 469.01 100%, M+1 470.10 24.3%, M-OCH_3 439, M-PhOCH_3 363,304, 203, 161 base peak. Anal. Calcd.for $C_{22}H_{19}N_3O_7$ S: C, 56.28; H, 4.08; N, 8.95; Found: C, 56.30;H, 4.06;N,8.91.

2-(2-(4-Chlorophenyl)-3-(2-(1,3-Dioxoisoindolin-2-yl)acetamido)-4-oxothiazolidin-5-yl)acetic acid (5g)

IR (KBr): *v*/cm^{-1}, 3540(OH of carboxyl), 3215(NH of amide), 3010 (C-H of aromatic), 2980(C-H of alkyl), 1755(C=O of thiazolidinone)1722(C=O of carboxyl), 1712, 1702 (C=O of Phthalimide), 1645(C=O of amide), 825(C-Cl),756(C-S). 1H NMR (CDCl3, 300 MHz) δ ppm: 10.23(s, 1H, -OH carboxyl), 8.48.(s, 1H, -NH), 7.16-7.81 (m, 8H, Ar-H), 6.36(s, 1H, -CH), 4.65 (s, 2H, -CH_2 near amide group),4.32(t, 1H, -CH), 2.61(d, 2H,CH_2), ^{13}CNMR (CDCl3, 300 MHz) δ ppm: 175.3 (carboxyl group),173.0(carbonyl of thiazolidinone ring), 170.3(carbonyl of amide), 168.2(two peaks carbonyl carbons of phthalimide ring), 137.3, 132.7, 132.0,131.8, 131.5, 130.1, 128.7, 123.7, (two aromatic rings carbon), 61.8 , 47.6 (-CH of thiazolidinone ring), 50.1 (-CH_2 near amide group) 39.2 (-CH_2 attached to carboxyl). MS m/z: M+ 473.04 100.0%, M+2 475.04 36.5%, M+1 474.05 23.1%, 161 base peak. Anal. Calcd. for $C_{21}H_{16}ClN_3O_6$ S: C, 53.22; H, 3.40; N, 8.87;Found: C, H, 3.43;N,8.91.

2-(3-(2-(1,3-Dioxoisoindolin-2-yl)acetamido)-2-(4-fluorophenyl)-4-oxothiazolidin-5-yl)acetic acid (5h)

IR (KBr): *v*/cm^{-1}, 3459(OH of carboxyl), 3314(NH of amide), 3042(C-H of aromatic),2890(C-H of alkyl),1758(C=O of thiazolidinone) 1735(C=O of carboxyl), 1712, 1710 (C=O of Phthalimide), 1680 (C=O of amide), 1329 (Ar-F), 736 (C-S).1H NMR (CDCl3, 300 MHz):.10.18(s, 1H, -OH carboxyl), 8.40.(s, 1H, -NH), 7.18-7.81 (m, 8H, Ar-H), 6.32(s, 1H, -CH thiazolodinone ring), 4.25(t, 1H, -CH thiazolodinone ring), 2.41(d, 2H,CH_2), ^{13}CNMR(CDCl3, 300 MHz) δ ppm: 175.3 (carboxyl group),173.0(carbonyl of thiazolidinone ring), 170.3(carbonyl of amide), 168.2(two peaks carbonyl carbons of phthalimide ring), 161.3, 134.8, 132.0,131.8, 131.5, 130.3, 128.7, 123.7, 115.4 (two aromatic rings carbon), 61.8 , 47.6 (-CH of thiazolidinone ring), 50.1 (-CH_2 near amide group) 39.2 (-CH_2 attached to carboxyl).MS m/z: M= 457.07 100.0%, M+1: 458.08 23.1%, 459.07 4.8%, 161 base peak .Anal. Calcd. for $C_{21}H_{16}FN_3O_6$ S: C, 55.14; H, 3.53; N, 9.19; Found: C,55.11;H,3.58; N,9.16.

2-(3-(2-(1,3-Dioxoisoindolin-2-yl)acetamido)-2-(3-nitrophenyl)-4-oxothiazolidin-5-yl)acetic acid (5i)

IR (KBr): *v*/cm^{-1}, 3546 (OH of carboxyl),), 3445(NH of amide), 3055 (CH of aromatic), 2936 (CH of alkyl), 1761(C=O of thiazolidinone), 1728, 1723 (C=O of Phthalimide), 1724(C=O of carboxyl) 1681 (C=O of amide), 1515(-NO_2), 737 (C-S), 1H NMR (DMSOd_6, 300 MHz):.11.1(s, 1H, -OH carboxyl), 8.42 (s, 1H, NH), 7.81 -

7.89(m, 4H, Ar- H), 6.23(s, 1H, -CH, thiazolidinone ring), 4.54 (s, 2H, $-CH_2$ near amide group) 4.35(t, 1H, -CH thiazolidinone ring), 2.81(d, 2H,CH_2),), ^{13}CNMR(CDCl3, 300 MHz) δ ppm: 175.3 (carboxyl group),173.0(carbonyl of thiazolidinone ring), 170.3(carbonyl of amide), 168.2(two peaks carbonyl carbons of phthalimide ring), 147.8, 140.1, 133.0, 132.2 132.0, 125.1, 123.7, 122.3 (two aromatic rings carbon), 60.8 , 47.6 (-CH of thiazolidinone ring), 50.1 ($-CH_2$ near amide group) 39.2 ($-CH_2$ attached to carboxyl).MS m/z::484.07 100.0%, 485.07 25.3%, 486.06 4.5 %, 161 base peak. Anal. Calcd. for $C_{21}H_{16}N_4O_8$ S: C, 52.07; H, 3.33; N, 11.57;Found: C, 52.03; H,3.30; N, 11.54.

2-(3-(2-(1, 3-Dioxoisoindolin-2-yl) acetamido)-2-(furan-2-yl)-4-oxothiazolidin-5-yl) acetic acid (5j)

IR (KBr): v/cm^{-1}, 3516 (OH of carboxyl), 3435(NH of amide), 3068 (CH of aromatic), 2945 (CH of alkyl), 1764(C=O of thiazolidinone), 1728, 1725 (C=O of Phthalimide), 1724(C=O of carboxyl) 1681 (C=O of amide), 737 (C-S), 1H NMR (CDCl3, 300 MHz): 11.1(s, 1H, -OHcarboxyl), 9.56 (s, 1H,NH), 7.81-7.89 (m, 4H, Ar-H), 6.07-7.09 (m, 3H, furan ring) 6.32(s, 1H, -CH), 4.61 (s, 2H, $-CH_2$) 4.25(t, 1H, -CH), 2.41(d, 2H,$CH_{2,}$ ^{13}CNMR (CDCl3, 300 MHz) δ ppm: 175.3 (carboxyl group),173.0(carbonyl of thiazolidinone ring), 170.3(carbonyl of amide), 168.2(two peaks carbonyl carbons of phthalimide ring), 151.5, 142.1,132.2 132.0, 123.7,110.6, 107.0 (aromatic rings carbon and furan ring carbon), 61.5 , 45.1 (-CH of thiazolidinone ring), 50.1 ($-CH_2$ near amide group) 39.2 ($-CH_2$ attached to carboxyl).MS m/z: M+: 429.06 100%, M+1 430.07 21.0% 431.06 4.8%, 161 base peak . Anal. Calcd. for $C_{19}H_{15}N_3O_7$S: C, 53.14; H, 3.52; N, 9.79; Found: C,53.11; H, 3.56;N,9.75.

2-(3-(2-(1, 3-Dioxoisoindolin-2-yl) acetamido)-4-oxo-2-(thiophen-2-yl)thiazolidin-5-yl)acetic acid (5k)

IR (KBr): v/cm^{-1}, 3563(OH of carboxyl), 3325 (NH of amide), 3108 (CH of aromatic), 2852 (CH of alkyl), 1780 (C=O of thiazolidinone), 1735(C=O of carboxyl)1733,1721 (C=O of Phthalimide), 1688(C=O of amide), 785, 737 (C-S) 1H NMR (CDCl3, 300 MHz): 11.1(s, 1H, -OH), 7.81-7.89 (m, 4H, Ar-H), 7.36(s, 1H,NH), 6.07-7.09 (m, 3H,thiphene ring) 6.32(s, 1H, -CH thiazolidinone ring), 4.58 (s, 2H, $-CH_2$ near amide group) 4.25(t, 1H, -CH thiazolidinone ring), 2.81(d, 2H,CH_2), ^{13}CNMR(CDCl3, 300 MHz) δ ppm: 175.3 (carboxyl group),173.0(carbonyl of thiazolidinone ring), 170.3(carbonyl of amide), 168.2(two peaks carbonyl carbons of phthalimide ring), 139.4, 132.2 132.0, 127.0, 126.7, 125.5123.7, (aromatic rings carbon and thiphene ring carbon), 61.0 , 47.5 (-CH of thiazolidinone ring), 50.1 ($-CH_2$ near amide group) 39.2 ($-CH_2$ attached to carboxyl). MS m/z: M+ 445.04 100%, 446.04 23.5%, 447.04 10.9%,161 base peak . Anal. Calcd. for $C_{19}H_{15}N_3O_6$S: C, 51.23; H, 3.39; N, 9.43;Found:C, 51.20;H,3.36;N,9.39.

2-(3-(2-(1,3-Dioxoisoindolin-2-yl)acetamido)-2-(1H-indol-2-yl)-4-oxothiazolidin-5-yl)acetic acid (5l)

IR (KBr): v/cm^{-1}, 3540 (OH of carboxyl), 3396 (NH of indole), 3209 (NH of amide), 3015 (CH of aromatic), 2867 (CH of alkyl), 1768 (C=O of thiazolidinone), 1724, 1721 (C=O of Phthalimide), 1724(C=O of carboxyl) 1680 (C=O of amide), 732 (C-S). 1H NMR (CDCl3, 300 MHz): 11.1(s, 1H, -OH), 9.56 (s, 1H,NH),8.7(s, 1H, NH of indole) 7.81-7.89 (m, 4H, Ar-H), 6.07-7.09 (m, 4H, aromatic ring) 6.32(s, 1H, -CH), 4.61 (s, 2H, $-CH_2$) 4.25(t, 1H, -CH), 2.41(d, 2H,CH_2), ^{13}CNMR (CDCl3, 300 MHz) δ ppm: 175.3 (carboxyl group),173.0(carbonyl of thiazolidinone ring), 170.3(carbonyl of amide), 168.2(two peaks carbonyl carbons of phthalimide ring),136.6, 136.5, 132.2 132.0, 128.1, 123.7,121.7, 120.7, 119.8, 111.1 (aromatic rings carbon and indolyl ring carbon), 61.5 , 47.5 (-CH of thiazolidinone ring), 50.1 ($-CH_2$ near amide group) 39.2 ($-CH_2$ attached to carboxyl). MS m/z: M+ 478.09 100%, 479.10 25.3%, 480.10 4.9%, 161 base peak. Anal. Calcd. for $C_{23}H_{17}N_4O_6$ S: C, 57.73; H, 3.79; N, 11.71; Found: C, 57.76;H,3.75;N,11.68.

Biological activity

In our present study we have performed *in vitro* biological activity by protein denaturation method and *in vivo* activity by carrageenan induced rat paw edema method, using diclofenac as standard.

***In vitro* anti-inflammatory activity**

The synthesized compounds were screened for anti inflammatory activity by using inhibition of albumin denaturation technique. The standard drug and test compounds were dissolved 10 mg compound in DMF and diluted with phosphate buffer saline (pH 7.4) in such a way that concentration of DMF in all solutions was less than 2.5%. Test solution (1 ml, 100 µg/ml) was mixed with 1 ml of 1% albumin solution in phosphate buffer saline and incubated at 27 ± 1°C in an incubator for 15 min. Denaturation was induced by keeping the reaction mixture at 60± 1°C in a water bath for 10 min. After cooling, the turbidity was measured at 660 nm with UV visible spectrophotometer. Percentage of inhibition of denaturation was calculated from control where no drug was added. Each experiment was done in triplicate and average is taken. The diclofenac sodium was used as standard drug. The percentage of inhibition was calculated using the following formula:

$$\% \textbf{ Inhibition of denaturation} = [(\mathbf{Vt/Vc}) - \mathbf{1}] \times \mathbf{100}$$

Where, Vt = mean absorption of test compound, Vc = mean absorption of control.

In vivo anti-inflammatory activity

The animals were procured under the CPCSEA number CPCSEA/IAEC/Pharm.Chem/19/2012-13/77 approved by Institutional Animal Ethics Committee (IAEC). Swiss Albino rats (150 to 200 g) were supplied by Wockhardt Ltd Aurangabad. The animals were housed in stainless steel cages, divided into groups of five animals each and deprived of food but not water 24 h before the experiment. The anti-inflammatory activity of the compounds under investigation was studied using carrageenan-induced rat paw oedema.

A suspension of the test compounds 5 (a-l) and standard drug diclofenac in carboxy methyl cellulose (CMC) solution (0.5% w/v in water) was administered intraperitoneally in a dose level of 10 mg/kg. Control animals were treated similarly with CMC solution (0.5% w/v in water). After 1 h, 0.1 ml of freshly prepared 1% carrageenan solution was injected into the sub plantar region of the left hind paw of rats according to the method of Winter et al. (1962). The volume was measured before and after carrageenan treatment at 1, 2, 3, 6 h with the help of digital plethysmometer (Ugo Basil 7140, Italy). Paw edema volume was compared with vehicle control group and percent reduction was calculated by formula:

Paw enema = (Vc – Vt / Vc) × 100

Where Vc = paw volume of control group, Vt = paw volume of test group

Ulcerogenic toxicity study

Ulcerogenic toxicity study was performed with Wistar albino rats as per the protocol (Susan et al. 1993; Shoman et al., 2009). Adult Wistar albino rats were divided into different groups each containing five animals. Animals were deprived of food with no water 24 h before experiment. Ulcerogenic activity was evaluated after oral administration of suspension of standard drug and test compounds in carboxy methyl cellulose solution (0.5% w/v in water) in dose level of 100 mg/kg.

Control animals were treated similarly with carboxy methyl cellulose solution (0.5% w/v in water). After 5 h, rats were scarified by decapitation, the stomach were removed, collected, opened along the greater curvature, washed with water, and cleaned gently in saline solution. The stomach was stretched on a piece of foam core mat and the numbers of severity score were recorded.

Severity score: 0 = Normal colored stomach, 0.5 = Red coloration, 1 = Spot ulcer, 1.5 = Hemorrhagic streaks, 2 = Ulcers ≥ 3 but ≤ 5, 3 = ulcers > 5. Calculation:

$$UI = UN + US + UP \times 10^{-1}$$

Where, UI = ulcer index, UN = average of number of ulcers per animal, US = average of severity score, UP = percentage of animals with ulcer.

RESULTS AND DISCUSSION

Chemistry

The synthetic protocol employed for the synthesis of 2-(3-(2-(1, 3-dioxoisoindolin-2-yl) acetamido)-4-oxo-2-substituted thiazolidin-5-yl) acetic acid derivatives 5(a-l) is presented in Figure 1. In the first step, 2-(1, 3-dioxoisoindolin-2-yl) acetic acid 1 was synthesized by refluxing phthalic anhydride and glycine in glacial acetic acid. Ethyl 2-(1, 3-dioxoisoindolin-2-yl) acetate 2 was synthesized by refluxing 1 with conc. H_2SO_4 in ethanol for 2 h. 2-(1, 3-Dioxoisoindolin-2-yl) acetohydrazide, 3 was synthesized by stirring ethyl 2-(1,3-dioxoisoindolin-2-yl) acetate 2 with hydrazine hydrate at room temperature for about 1 h. The compounds N-substituted benzylidene/methylene-2-(1,3-dioxoisoindolin-2-yl) acetohydrazides 4(a-l) were synthesized by refluxing 2-(1,3-dioxoisoindolin-2-yl) acetohydrazide and aromatic/heterocyclic aldehydes in absolute ethanol in presence of catalytic amount of glacial acetic acid.

The title compounds 2-(3-(2-(1,3-dioxoisoindolin-2-yl) acetamido)-4-oxo-2-substituted thiazolidin-5-yl) acetic acid 5(a-l) were obtained by cyclo-condensation of *N*-substitutedbenzylidene/methylene-2-(1,3-dioxoisoindolin-2-yl)acetohydrazide with mercapto succinic acid in dimethylformamide (DMF) as solvent in presence of catalytic amount of anhydrous zinc chloride, under microwave irradiation for about 14 to 17 min (700 W) at 80°C. The reactions were carried out in microwave so as to reduce the longer reaction time of 6-8hrs refluxing in benzene, required in conventional synthesis of thiazolindinone derivatives to have better yields and to have neat and clean reactions. In the present synthesis of thiazolidinone derivatives the carcinogenic solvent benzene is replaced by DMF. The characterization data of synthesized derivatives is given in Table 1.

Biological activity

The synthesized derivatives 5(a-l) were evaluated for anti inflammatory activity using *in vitro* activity by protein denaturation method and *in vivo* activity was performed by using carageenan induced paw edema method. Diclofenac was used as the standard reference compound for both *in vivo* and *in vitro* evaluation.

The *in vivo* biological activity was performed according to Winter et al. (1962) and it has been observed that the new series of 2-(3-(2-(1,3-dioxoisoindolin-2-yl) acetamido)-4-oxo-2-substituted thiazolidin-5-yl) acetic acid derivatives exhibited the significant anti-inflammatory

Table 1. Physical data 2-(3-(2-(1,3-dioxoisoindolin-2-yl) acetamido)-4-oxo-2-substituted thiazolidin-5-yl)acetic acid.

Code	R/Ar	Molecular formula	Molecular weight	% Yield	MP (°C)	R_f value
5a	—CH_3	$C_{16}H_{15}N_3O_6S$	377	89	280-284	0.63
5b	—CH_2CH_3	$C_{17}H_{17}N_3O_6S$	391	93	298-302	0.56
5c	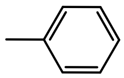	$C_{21}H_{17}N_3O_6S$	439	98	310-312	0.56
5d	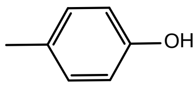	$C_{21}H_{17}N_3O_7S$	455	90	300-302	0.61
5e	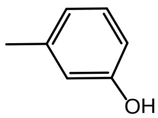	$C_{21}H_{17}N_3O_7S$	455	85	320-322	0.48
5f	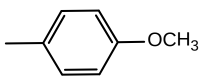	$C_{22}H_{19}N_3O_7S$	469	95	270-273	0.45
5g	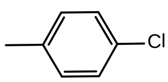	$C_{21}H_{16}ClN_3O_6S$	473	94	312-316	0.61
5h	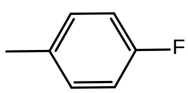	$C_{21}H_{16}FN_3O_6S$	457	93	273-276	0.53
5i	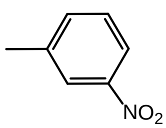	$C_{21}H_{16}N_4O_8S$	484	89	298-300	0.52
5j	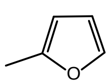	$C_{19}H_{15}N_3O_7S$	429	88	304-306	0.49
5k	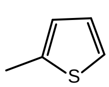	$C_{19}H_{15}N_3O_6S$	445	98	284-288	0.39
5l	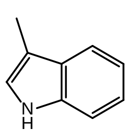	$C_{23}H_{17}N_4O_6S$	478	90	312-318	0.67

*Melting points are uncorrected

Table 2. Mean paw volume (ml) and % inhibition of compounds (5a-l).

No.	Mean paw volume in ml ± SEM					% inhibition				
	1 h	2 h	3 h	4 h	6 h	1 h	2 h	3 h	4 h	6 h
Control	1.34±0.15	1.53±0.017	1.926±0.15	1.776±0.061	1.856±0.053	-	-	-	-	-
5a	0.7±0.30**	0.91±0.069*	0.846±0.037	1.243±0.098	1.433±0.19	47.76	87.58	50.07	30.01	22.79
5b	1.023±0.038	0.88±0.017	0.97±0.011	1.153±0.075	1.33±0.050	23.65	42.48	49.63	35.07	28.34
5c	1.29±0.084	0.96±0.04	1.09±0.005**	1.243±0.035	1.19±0.078	3.7	37.25	43.40	30.01	35.88
5d	1.26±0.072	1.216±0.029	1.42±0.14**	1.43±0.12*	1.286±0.10	5.9	20.52	26.27	19.48	30.71
5e	0.91±0.07	1.06±0.060	1.296±0.046	1.13±0.047	1.346±0.069	32.08	30.71	32.71	36.37	27.47
5f	1.29±0.04	1.253±0.089	1.12±0.10**	1.61±0.065	1.4±0.061	3.7	18.10	41.84	9.34	24.56
5g	0.96±0.037	1.22±0.058	1.34±0.14*	1.003±0.093**	1.06±0.06	28.35	20.26	30.42	43.52	42.88
5h	1.223±0.017	1.013±0.080*	1.43±0.052*	1.123±0.035**	1.583±03031	8.73	33.79	25.75	36.76	14.70
5i	1.143±0.086	1.11±0.055	1.333±0.071**	1.38±0.127	1.113±0.014	14.70	64.26	30.94	22.29	40.03
5j	0.896±0.031	1.366±0.023	1.1±0.10**	1.206±0.053	1.22±0.11	33.13	10.71	42.88	32.09	32.26
5k	1.22±0.035	1.29±0.036	1.496±0.139	1.256±0.089	1.486±0.069	8.95	15.66	22.32	29.27	19.93
5l	1.25±0.075	1.33±0.75	1.556±0.15	1.273±0.72	1.643±0.68	6.7	13.07	19.21	28.32	11.47
Diclofenac	1.123±0.16	1.056±0.99	1.156±0.098**	1.133±0.021**	1.36±0.033	16.19	30.98	39.97	36.20	26.72

The observations are mean ± SEM, n= 5, ***P* < 0.01, **P* < 0.05, test compounds = 10 mg/kg. Reference standard, Diclofenac = 10 mg/kg. Statistical analysis were done by one way ANOVA followed by Dunnett's test

action to all the compounds except 5b , 5k and 5l, when compared with control. Some of the synthesized derivatives have shown the enhanced anti-inflammatory activity than diclofenac as shown in Table 2. The most significant (***P* < 0.01) anti-inflammatory activity is foundat 3 h and gradually reduces at subsequent hours. The compound with highest percent inhibition is 5a and is found to be most significant at 1 h. From the overall percent inhibition the compound 5c, 5f and 5j have shown to posses the enhanced and significant anti-inflammatory activity. Moreover, the other derivatives are also significant but less or equipotent with the standard drug, diclofenac.

The synthesized compound were subjected to *in vitro* anti inflammatory activity using albumin inhibition of albumin denaturation technique according to (Mizushima and Kobayashi. 1968), and with slight modification according to Bhalgat et al. 2011. Amongst all the synthesized compounds 5a, 5b and 5e have shown more inhibition as compared to diclofenac. It was observed in *in-vivo* activities, that lower aliphatic groups such as–CH_3, -C_2H_5 attached to C2 of thiazolidinone ring show the highest anti-inflammatory activity. All the compounds have resulted in decrease in rat paw edema and hence showed excellent anti-inflammatory activity. Compound 5c in which the phenyl ring is without any substituent attached at C2 of thiazolidinone ring exhibited significant and enhanced anti-inflammatory activity. Other derivatives possessing 4-nitro phenyl, 4-fluro phenyl, 4-chloro phenyl, 3- hydroxy phenyl, 4-hydroxy phenyl group on C2 of thiazolidinone ring ie. 5i, 5h, 5g, 5e, 5d, respectively are less active than diclofenac but show significant activity. The bulky derivatives such as indole and thiophene rings at C2 of thiazolidinone ring like 5k and 5l have exhibited very less anti-inflammatory activity when compared to the standard drug, diclofenac. The anti-inflammatory activity data is presented in Table 3. The ulcerogenic toxicity was performed for selected compounds having shown better anti-inflammatory activity, such as, compound 5a, 5b, 5c, 5f & 5j. As shown in Table 4, it was observed that all the compounds exhibited lesser ulcerogenic index than diclofenac. Thus the synthesized derivatives have shown minimum toxicity effects.

Docking methodology

Molecular docking studies were performed by using Glide, V 5.5 (Schrödinger. LLC, New York, NY 2009). The coordinates for HSA were taken from RCSB Protein Data Bank (PDB Id. 2BXQ) (Ghuman et al., 2005) and prepared for docking using protein preparation wizard. Water molecules in the structure were removed. The bond order and formal charges were added for hetero groups and the hydrogens were added to all atoms in the structure. Side chains that were not close to the binding cavity were removed. After preparation, the structures were refined to optimize the hydrogen bond network using OPLs_2005 force field which helps in the orientation of side chain hydroxyl group. The minimization was terminated when the energy converged to root-mean-square deviation (RMSD) reached a maximum cutoff of 0.30A°. Grids were then defined around refined structure by centering on ligand using default box size. The standard precision (SP) docking mode for compounds, optimized earlier by Ligprep, was performed on generated grid of protein structure.

Table 3. Mean absorbance± SEM and % inhibition of compounds (5a-5l).

Compound	Mean Absorbance	SEM	% Inhibition
Control	0.1023	0.060	-
5a	0.1890	0.026	84.75
5b	0.1784	0.014	74.38
5c	0.1501	0.03	46.72
5d	0.1212	0.02	18.96
5e	0.1697	0.020	65.88
5f	0.1091	0.015	6.64
5g	0.1276	0.015	24.73
5h	0.1289	0.014	26.00
5i	0.1346	0.30	31.57
5j	0.1566	0.15	53.07
5k	0.1493	0.2	45.94
5l	0.1176	0.026	14.95
Std (diclofenac sodium)	0.1673	0.019	63.53

Table 4. Ulcerogenic potential in rat stomach.

Group	Dose mg/kg	Ulcer index
Control	0.5% sodium CMC	0
Diclofenac	100	11.4 ± 0.2082
5a	100	3.348 ± 0.0833
5b	100	7.21 ± 0.02887
5c	100	4.13 ± 0.04410
5f	100	4.66 ± 0.0333
5j	100	6.15 ± 0.05774

The observations are mean ± SEM, n= 6, ** $P < 0.01$, * $P < 0.05$. Test compounds = 100 mg/kg. Reference standard, Diclofenac = 100 mg/kg. Statistical analysis were done by one way ANOVA followed by Dunnett's test.

Docking results

While performing docking study the hydrogen bonding with ARG114 was selected as constraints for the specificity of binding of compounds in activity site of enzyme as reported in literature and as detected in Ligplot (Pawar et al., 2010). The docking pose of synthesized compounds showing higher inhibition compared with that of standard. In present docking study both the standard drug Indomethacin shows the binding with Arg114 (Figure 2) and diclofenac shows the binding with Arg 117, as found in Figure 3. The compound 5a and 5b shows binding with ARG114 and ARG117, as shown in Figure 4 and Figure 5, respectively. Moreover the compound 5a showed the highest G score of -7.731, it was observed in the docking pose of 5a that –C=O of carboxyl group formed hydrogen bonding with –-NH group of Arg186 and –NH of amide group formed hydrogen bonding with –C=O of Arg114. This indicates the importance of carboxyl group for anti-inflammatory activity and also confirms the importance of amide group in the structure of the synthesized derivatives. The docking results have shown that all the synthesized compounds have better anti inflammatory effect compared to Indomethacin and diclofenac. Molecular modeling helps to realize the mechanism of their actions, which could be their interactions with the same residues of ARG114 and ARG117, as shown by indomethacin and diclofenac.

Conclusion

The present study describes eco-friendly synthesis of twelve final derivatives 5(a-l) in Milestone's Microsynth microwave. All the compounds were obtained in good yield and in shorter reaction times, i.e. 14 to 17 min.

The synthesized derivatives were evaluated for *in vitro*

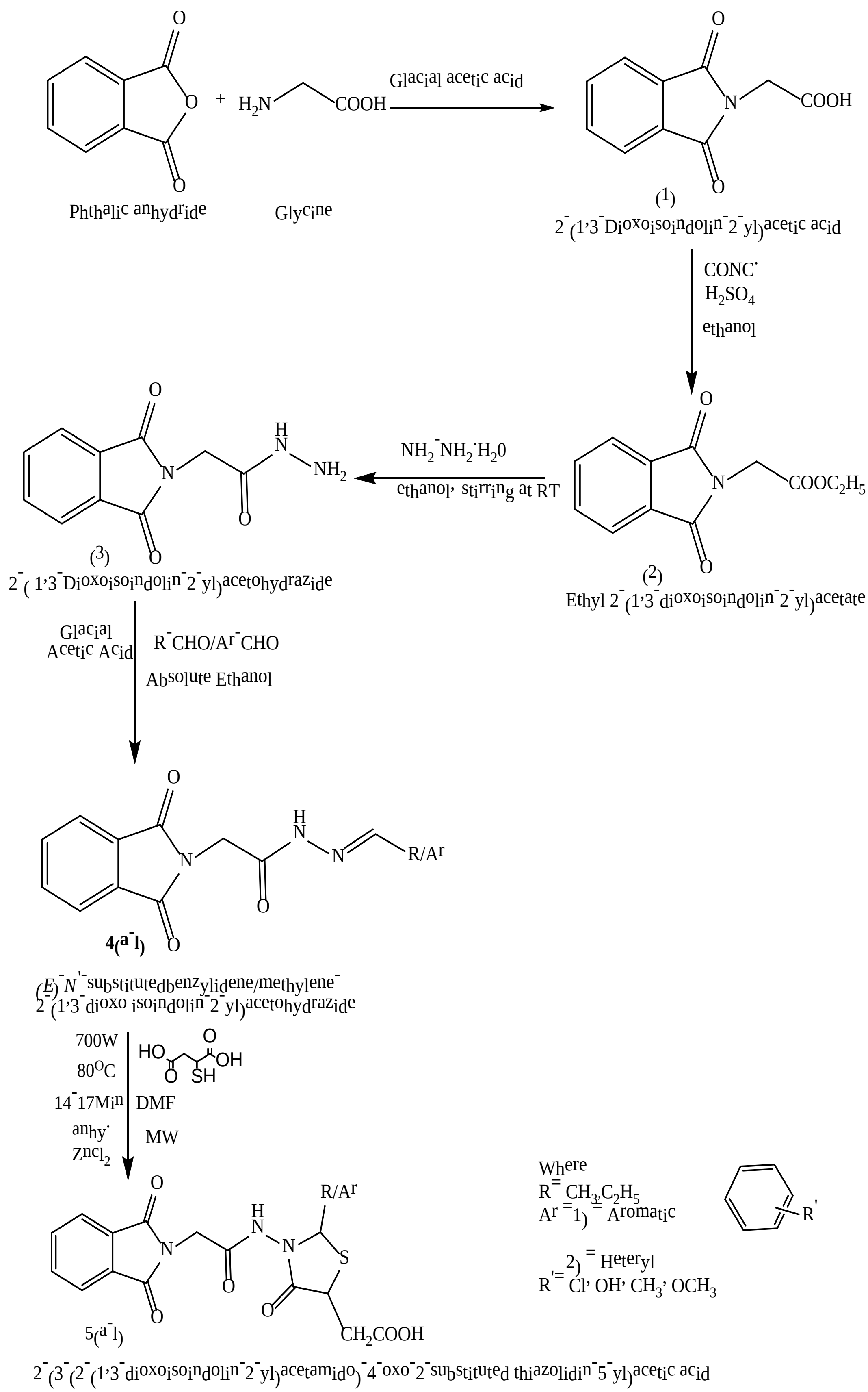

Figure 1. Scheme of synthesis of 2-(3-(2-(1,3-Dioxoisoindolin-2-yl) acetamido)-4-oxo-2-substituted thiazolidin-5-yl)acetic acid.

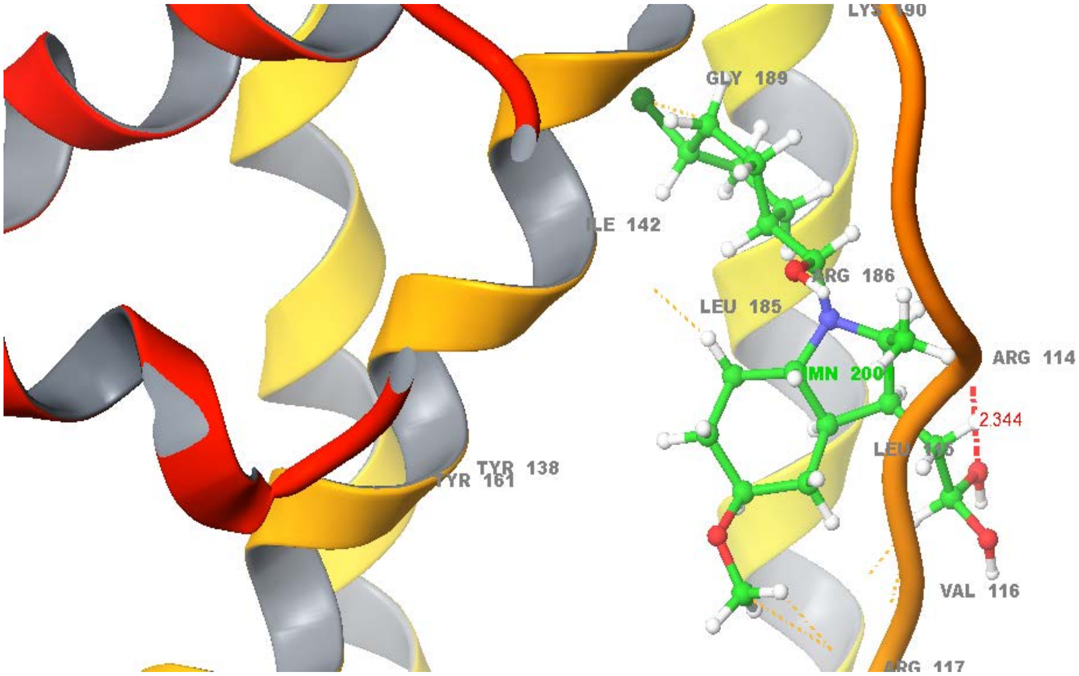

Figure 2. Docking pose of compound indomethacin at active binding site of enzyme. Visualization of hydrogen bonding of Indomethacin with Arg114 and Arg186.

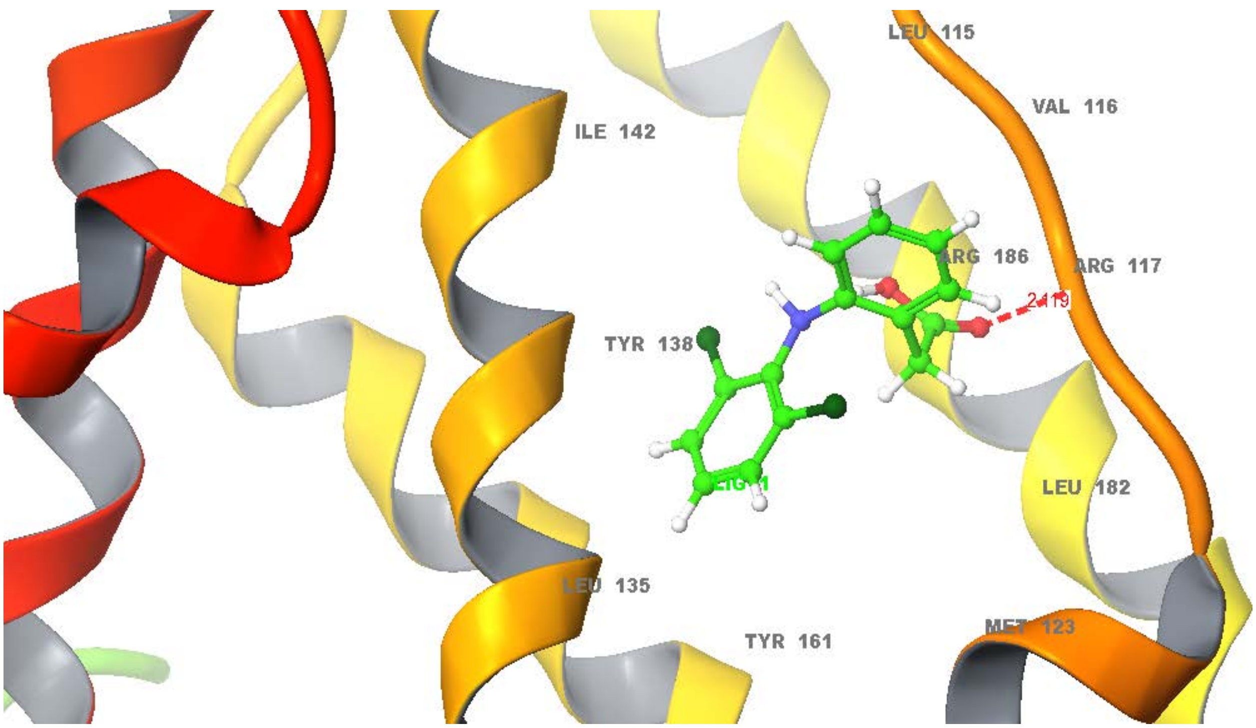

Figure 3. Docking pose of compound diclofenac at active binding site of enzyme. Visualization of hydrogen bonding of diclofenac with Arg117 (hydrogen bonding with amino acid is shown in pink dotted lines).

and *in vivo* anti-inflammatory activity, using diclofenac as a reference standard. The selected compounds were studied for ulcerogenic toxicity and have shown good gastrointestinal safety profile. The compounds were also subjected to *in vitro* analysis by using diclofenac as standard. The compounds 5a, 5b and 5e have proved to

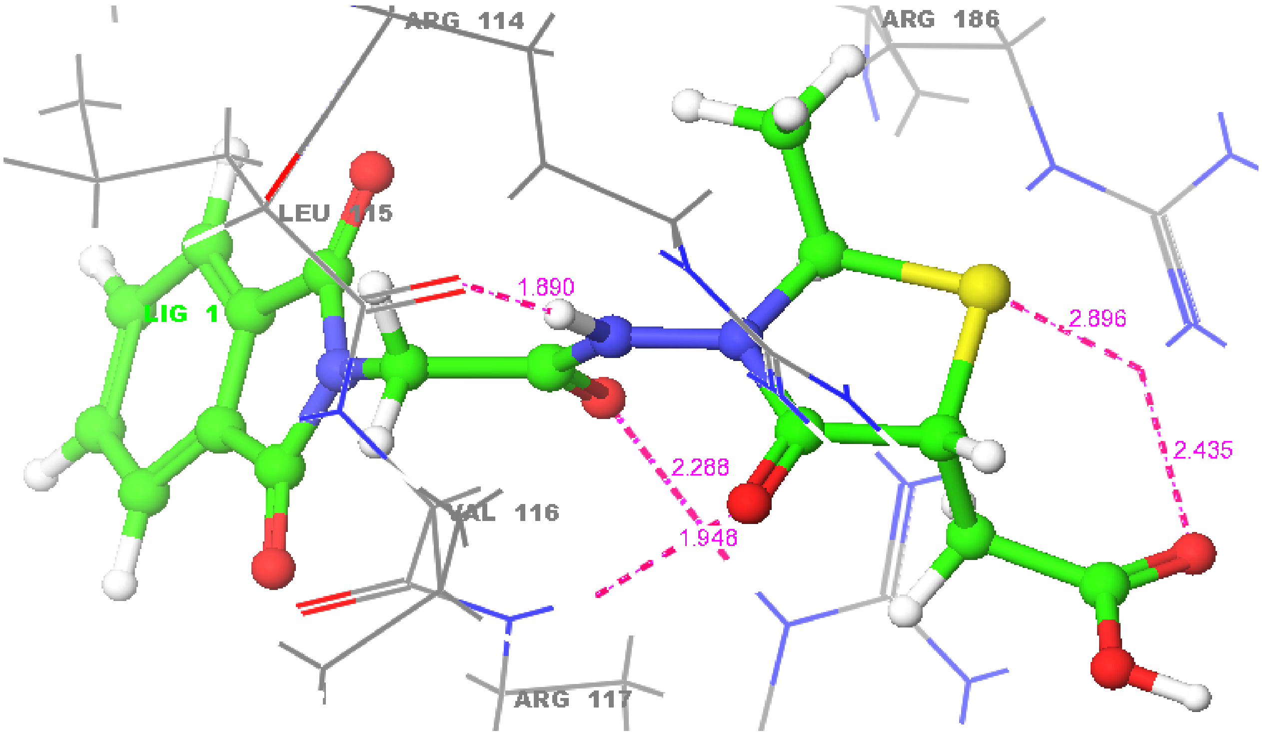

(a)

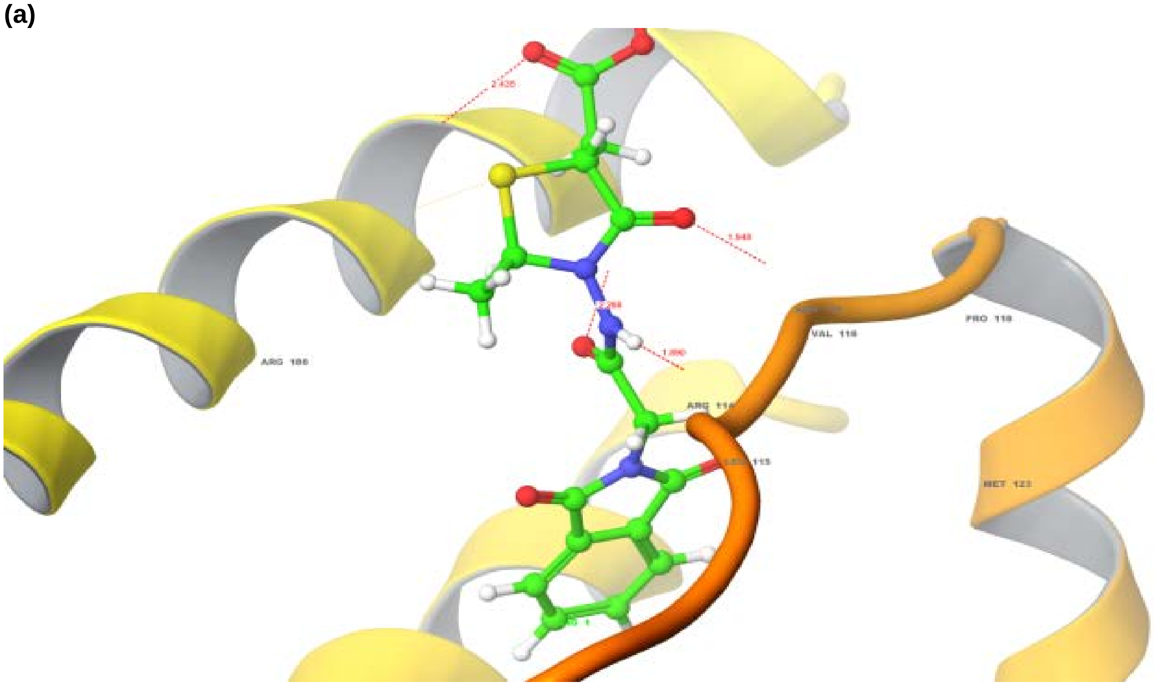

(b)

Figure 4. Docking pose of compound (5a) at active binding site of enzyme. Visualization of hydrogen bonding of (5a) with Arg114, Arg117 and Arg186. Hydrogen bonding with amino acid is shown in pink dotted lines.

be more effective than diclofenac while others have shown moderate to weak activity. All the derivatives were fitted into the same pocket of HSA where indomethacin has fitted during docking. The compounds have shown good docking results (G-score) and good fitting into the active site. Thus the synthesized compounds 2-(3-(2-(1,3-dioxoisoindolin-2-yl) acetamido)-4-oxo-2-substituted thiazolidin-5-yl) acetic acid derivatives 5(a-l) show good potential as anti-inflammatory agents and can be further evaluated for diabetic neuropathy as the structure

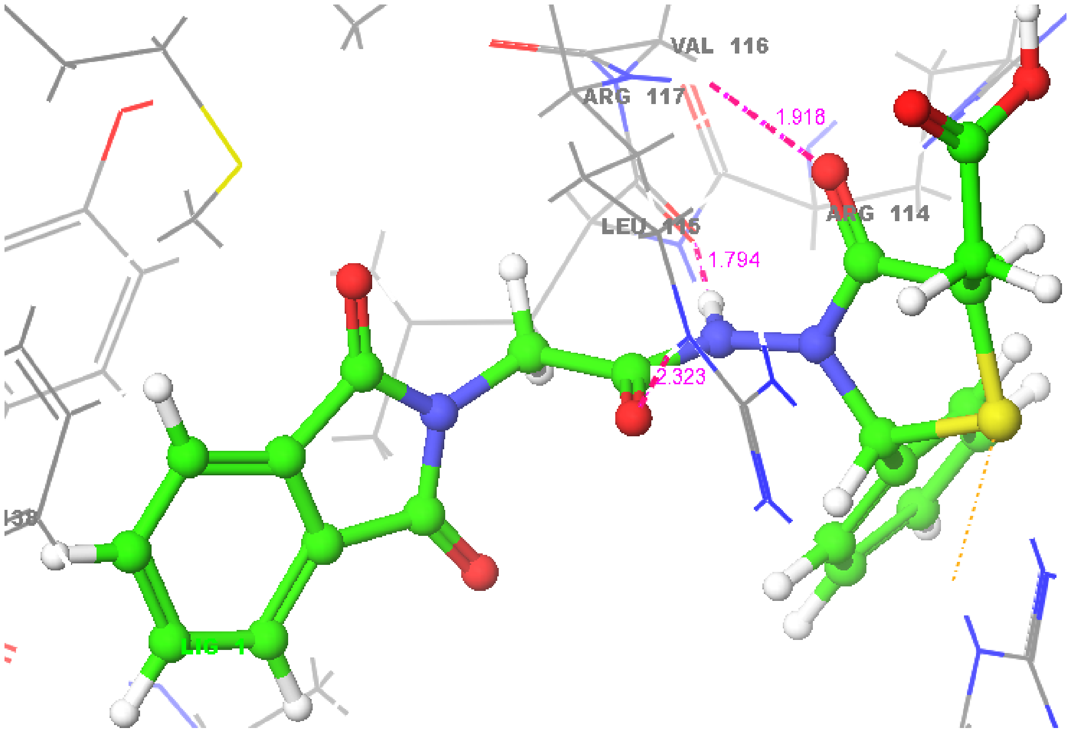

Figure 5. Docking pose of compound (5b) at active binding site of enzyme. Visualization of hydrogen bonding of (5b) with Arg114, Arg117. Hydrogen bonding with amino acid is shown in pink dotted lines.

contains thiazolidinone ring which is also present in anti-diabetic drugs such as rosiglitazone and pioglitazone.

ACKNOWLEDGMENTS

Authors are grateful to Mrs. Fatma Rafiq Zakaria, Chairman, Maulana Azad Education Trust and Principal, Y.B Chavan College of Pharmacy, Aurangabad for encouragement and support. The authors thank the Government College of Pharmacy, for assisting in pharmacological screening.

Conflict of interest

The authors declared no conflict of interest.

REFERENCES

Ahmed O, Salahuddin M, Rizwana I, Aleem M, Sharma P (2013). Synthesis, Characterization and Biological Evaluation of Novel thiazolidinone Derivatives as Anti-Inflammatory Agents. IAJPR, 3(10):8121- 8126.

Alanazi AM, El-Azab AS, Al-Suwaidan IA, Tahir KE, Asiri YA, Aziz NI, Abdel A (2015). Structure-Based Design of Phthalimide Derivatives as Potential Cyclooxygenase-2 (COX-2) Inhibitors: Anti-Inflammatory and Analgesic Activities. Eur. J. Med. Chem. 92: 514-530.

Amin KM, Kamel MM, Anwar MM (2010). Synthesis, Biological Evaluation and Molecular Docking of Novel Series of Spiro [(2H,3H) Quinazoline-2,1'- Cyclohexan]-4(1H)- One Derivatives as Anti-Inflammatory and Analgesic Agents. Eur. J. Med. Chem. 45:2117–2131.

Amir M, Shikha K (2004). Synthesis and Anti-Inflammatory, Analgesic, Ulcerogenic and Lipid Peroxidation Activities of some New 2-[(2,6-Dichloroanilino) Phenyl]Acetic Acid Derivatives. Eur. J. Med. Chem. 39: 535–545.

Balzarini J, Orzeszko B, Maurin JK, Orzeszko A (2007). Synthesis and Anti-HIV Studies of 2-Adamantyl-Substituted Thiazolidin-4-Ones. Eur. J. Med. Chem. 42:993-1003.

Bhalgat CM, Sangeetha M, Soni BK, Singh T, Mudshinge SR (2011). In-vitro Anti-Inflammatory Studies of 3-(1-Benzofuran-2-yl)-5-(substituted aryl) isoxazole. Int. J. Res. Pharm. Biomed. Sci. 2:1203.

Bhat S, Kumar A (2008). Synthesis Of New Substituted Azetidinoyl And Thiazolidinoyl-1,3,4-Thiadiazino (6,5-B) Indoles as Promising Anti-Inflammatory Agents. Eur. J. Med. Chem. 43:2323-2330.

Bosquesi PL, Ferreira TR, Vizioli EO, Santos JL, Chung MC (2011). Anti-Inflammatory Drug Design Using a Molecular Hybridization Approach. Pharmaceuticals (2011), 4, 1450-1474.

Furniss B, Hannaford AH, Smith PWG (1998). Vogel's Text book of Practical Organic Chemistry. 15:1077.

Susan G, Anuradha S, Sathiamoorthy SS (1999). Effect of alpha tocopherol on gastric ulcers induced by pylorus ligation in rats. Indian J. Pharmacol. 31(6):431.

Ghuman J, Zunszain PA, Petitpas I, Bhattacharya AA, Otagiri M, Curry S (2005). Structural basis of the drug-binding specificity of human serum albumin. J. Mol. Biol. 353:38-52.

Gududuru V, Hurh E, Dalton JT, Miller DD (2004). Synthesis and antiproliferative activity of 2-aryl-4-oxo-thiazolidin-3-yl-amides for prostate cancer. Bioorg. Med. Chem. Lett. 14:5289.

Hu J, Wang Y, Wei X, Wu X, Chen G, Cao G, Shen X, Zhang X, Tang Q, Liang G (2013). Synthesis and biological evaluation of novel thiazolidinone derivatives as potential anti-inflammatory agents. Eur J Med Chem. 64:292-301.

Jackson CM, Blass B, Coburn K, Djandjighian L, Fadayel G, Fluxe AJ, Hodson SJ, Janusz JM, Murawsky M, Ridgeway JM, White RE, Wu S (2007). T3P Ò -DMSO mediated one pot cascade protocol for the synthesis of 4-thiazolidinones from alcohols. Bioorg. Med. Chem. Lett. 17 (2007):282.

Lombardino JG (1985). Medicinal Chemistry of Acidic Nonsteroidal Antiinflammatory Drugs. In: Lombardino JG (Ed.), Nonsteroidal Antiinflammatory Drugs. Wiley-Interscience, New York. P 255.

Machado AL, Lima LM, Araújo JX, Fraga CA, Koatz VL (2005). Design, synthesis and antiinflammatory activity of novel phthalimidederivatives, structurally related to thalidomide. Bioorg. Med. Chem. Lett. 15(4):1169-72.

Madhukar M, Sawraj S, Sharma PD (2010). Design, synthesis and evaluation of mutual prodrug of 4-biphenylacetic acid and quercetin tetramethyl ether (BPA–QTME) as gastrosparing NSAID. Eur. J. Med. Chem. 45(6):2591-2596.

Mizushima Y, Kobayashi M (1968). Interaction of anti-inflammatory drugs with serum proteins, especially with some biologically active proteins. J. Pharm. Pharmacol. 20(3):169-173.

Monforte P (2001). Discovery of 2,3-diaryl-1,3-thiazolidin-4-ones as potent anti-HIV-1 agents. Bioorg. Med. Chem. 11:1793–1796.

Ottana R, Maccari R, Barreca ML (2005). 5-Arylidene-2-imino-4-thiazolidinones: design and synthesis of novel anti-inflammatory agents. Bioorg. Med. Chem. 13:4243–4252.

Pawar P, Chavan M (2012). Synthesis and Pharmacological Evaluation of 1, 3-Isoindolinedione Derivatives as Analgesic and Antiinflammatory Agents. Asian J. Res. Chem. 5:127-130.

Pawar V, Lokwani D, Bhandari S, Mitra D, Sabde S, Bothara K, Madgulkar A (2010). Design of potential reverse transcriptase inhibitor containing Isatin nucleus using molecular modeling studies Bioorg. Med. Chem 18:3198-3211.

Pilotto A, Franceschi M, Leandro G, Dimario F, Valerio G (1997). The effect of *Helicobacter pylori* infection on NSAID-related gastroduodenal damage in the elderly. Eur. J. Gastroenterol. Hepatol. 9(10):951-6.

Pirson Y, Van DE, Strihou C (1986). Renal side effects of nonsteriodal anti-inflammatory drugs: clinical relevance. Am. J. Kidney Dis. 8(5):338-44.

Pophale RA, Deodhar MN (2010). Synthesis and evaluation of novel phthalimide derivatives as analgesic and antiinflammatory agents. Pharm. Chem. 2(1):185-193.

Shoman ME, Abdel-Aziz M, Aly OM, Farag HH, Morsy MA (2009). Synthesis and investigation of anti-inflammatory activity and gastric ulcerogenicity of novel nitricoxide-donating pyrazoline derivatives. Eur. J. Med. Chem. 44(7):3068-76

Singh N, Tripathi A, Tewari A, Kumar R, Saraf S (2014). Ulcerogenicity devoid novel non-steroidal anti-inflammatory agents (NSAIDS): syntheses, computational studies, and activity of 5-aryliden-2-imino-4-thiazolidinones. Med. Chem. Res. 23(9).

Solomon VR, Haq W, Srivastava K, Puri SK, Katti SB (2013). Design, synthesis of 4-aminoquinoline-derived thiazolidines and their antimalarial activity and heme polymerization inhibition studies. J. Med. Chem. 50:394.

Thomas AB, Nanda RK, Kothapalli LP, Sharma PA, Apte KG (2013). Synthesis, Biological Activity, Molecular Modelling Studies and 3D-QSAR Investigations of N-[2-(aryl/substituted aryl)-4-oxo-1, 3-thiazolidin-3-yl] pyridine-4-carboxamides. Open Conf. Proc. J. 4:99-112.

Unsal T, Ozadali K, Piskin K (2012). Molecular modeling, synthesis and screening of some new 4-thiazolidinone derivatives with promising selective COX-2 inhibitory activity. Eur. J. Med. Chem. 57:59-64.

Vigorita MG, Ottana R, Monforte R (2002). Modeling and biological evaluation of 3,3′-(1,2-ethanediyl)bis[2-(4-methoxyphenyl)-thiazolidin-4-one], a new synthetic cyclooxygenase-2 inhibitor. Eur. J. Pharm. 448:71-80.

Winter CA, Risley EA, Nuss GW (1962). Carrageenin-induced edema in hind paw of the rat as an assay for anti-inflammatory drugs. Proc. Soc. Exp. Biol. Med. 111(1962) 544-547.


African Journal
of Pharmacy and
Pharmacology
Related Journals Published by Academic Journals
■ Journal of Medicinal Plant Research
■ African Journal of Pharmacy and Pharmacology
■ Journal of Dentistry and Oral Hygiene
■ International Journal of Nursing and Midwifery
■ Journal of Parasitology and Vector Biology
■ Journal of Pharmacognosy and Phytotherapy
■ Journal of Toxicology and Environmental Health Sciences
academicJournals